

Penalized Orthogonal Iteration for Sparse Estimation of Generalized Eigenvalue Problem

Sungkyu Jung

Department of Statistics, University of Pittsburgh

Jeongyoun Ahn

Department of Statistics, University of Georgia

and

Yongho Jeon

Department of Applied Statistics, Yonsei University

June 29, 2018

Abstract

We propose a new algorithm for sparse estimation of eigenvectors in generalized eigenvalue problems (GEP). The GEP arises in a number of modern data-analytic situations and statistical methods, including principal component analysis (PCA), multiclass linear discriminant analysis (LDA), canonical correlation analysis (CCA), sufficient dimension reduction (SDR) and invariant co-ordinate selection. We propose to modify the standard generalized orthogonal iteration with a sparsity-inducing penalty for the eigenvectors. To achieve this goal, we generalize the equation-solving step of orthogonal iteration to a penalized convex optimization problem. The resulting algorithm, called penalized orthogonal iteration, provides accurate estimation of the true eigenspace, when it is sparse. Also proposed is a computationally more efficient alternative, which works well for PCA and LDA problems. Numerical studies reveal that the proposed algorithms are competitive, and that our tuning procedure works well. We demonstrate applications of the proposed algorithm to obtain sparse estimates for PCA, multiclass LDA, CCA and SDR. Supplementary materials are available online.

Keywords: Canonical correlation analysis, Classification, Group lasso, Lasso, Eigen-decomposition, Principal component analysis, Sufficient dimension reduction.

1 Introduction

Many statistical problems can be cast into the mathematical framework of a generalized eigenvalue problem (GEP). In particular, we focus on the symmetric-definite GEP, posed as follows. Suppose that $\mathbf{A} \in \mathbb{R}^{p \times p}$ is a symmetric matrix, and $\mathbf{B} \in \mathbb{R}^{p \times p}$ is a symmetric positive-definite matrix. While specific statistical contexts determine the exact nature of \mathbf{A} and \mathbf{B} , a solution of GEP is given by a d -dimensional subspace \mathcal{U}_d that is spanned by the generalized eigenvectors $\mathbf{u}_1, \dots, \mathbf{u}_d$ corresponding to the d largest generalized eigenvalues. The following equations define a generalized eigen-pair $(\lambda_j, \mathbf{u}_j)$:

$$\mathbf{A}\mathbf{u}_j = \lambda_j\mathbf{B}\mathbf{u}_j, \tag{1}$$

where the generalized eigenvalues, $\lambda_1 \geq \dots \geq \lambda_d$, satisfy $\lambda_j = \mathbf{u}_j^T \mathbf{A} \mathbf{u}_j / \mathbf{u}_j^T \mathbf{B} \mathbf{u}_j$. The generalized eigenvectors are orthogonal with respect to \mathbf{B} , i.e., $\mathbf{u}_i^T \mathbf{B} \mathbf{u}_j = 1$ for $i = j$, and 0 for $i \neq j$. In the special case of $\mathbf{B} = \mathbf{I}_p$, the GEP is the standard eigenvalue problem.

Immediate applications of the GEP are to multivariate analysis problems, including the principal component analysis (PCA), canonical correlation analysis (CCA), multiclass linear discriminant analysis (LDA), invariant co-ordinate selection (Tyler et al., 2009) and sufficient dimension reduction (Li, 2007). The GEP also appears frequently in nonlinear dimension reduction (Kokopoulou et al., 2011) and in computer vision and image processing (Zhang et al., 2013). We refer to the online supplementary material for detailed description of some selected statistical GEP problems.

When p is large, it is often desirable to find a sparse representation of \mathcal{U}_d , so that its basis vectors are sparse, i.e., the vectors have many zero loadings in their entries. We propose an efficient algorithm for estimating sparse generalized eigenvectors from noisy observations of \mathbf{A} and \mathbf{B} . It is well-known that in the standard eigenvalue problem, e.g. for PCA, the standard eigenvectors of the sample covariance matrix \mathbf{A} (while $\mathbf{B} = \mathbf{I}_p$) is inconsistent with the true principal directions for large p (Johnstone and Lu, 2009; Jung and Marron, 2009). Thus in the high-dimension, low-sample-size situations, sparsity-inducing methods have a potential in improving the estimation accuracy, as well as in providing interpretable eigenvectors through variable selection.

Our approach to obtain a sparse solution of the GEP is to extend the generalized or-

thogonal iteration, a standard numerical method of solving the GEP (Golub and Van Loan, 1996). The generalized orthogonal iteration consists of iterating two steps: one involving solutions of linear equations, and an orthogonalization step. One of our main ideas is to transform the equation-solving step to a minimization of a quadratic objective function, so that a sparsity-inducing penalty can be easily incorporated. We propose to use ℓ_1 -norm or $\ell_{2,1}$ -norm penalty on the eigenvector matrix to induce element-wise or coordinate-wise sparsity. These penalty functions are those used in lasso and group-lasso regressions (*cf.* Hastie et al., 2009). The proposed method is called *Penalized Orthogonal Iteration* (POI). We utilize the block coordinate descent algorithm in solving the penalized minimization problem at each iteration. We also study a computationally efficient alternative to POI, that comes down to solving just one minimization problem. We establish sufficient conditions under which the solutions of this alternative method, called *Fast POI*, correspond to the solutions of the GEP. The conditions are satisfied under the situations for PCA and multiclass LDA.

The solutions of POI and Fast POI depend on the choice of a tuning parameter, dictating the degrees of penalization. Larger values of the tuning parameter result in more sparse solutions of the generalized eigenvectors. When the tuning parameter is zero, POI becomes the generalized orthogonal iteration. An eigenvalue-based cross-validation procedure is proposed, and is seen to work well in numerical studies.

To the best of authors' knowledge, there have been only a few proposals for sparse GEP in the literature (Sriperumbudur et al., 2011; Song et al., 2015; Tan et al., 2016; Gaynanova et al., 2017; Han and Clemmensen, 2016; Safo et al., 2018). We briefly discuss their approaches and limitations, compared to our proposal.

Since finding the largest eigenvalue λ_1 that solves (1) is equivalent to maximize $\mathbf{u}^T \mathbf{A} \mathbf{u}$ subject to $\mathbf{u}^T \mathbf{B} \mathbf{u} = 1$, Sriperumbudur et al. (2011) formulated both an ℓ_0 -constrained GEP and an ℓ_0 -penalized GEP:

$$\max_{\mathbf{u}} \mathbf{u}^T \mathbf{A} \mathbf{u}, \quad \text{subject to } \mathbf{u}^T \mathbf{B} \mathbf{u} = 1, \|\mathbf{u}\|_0 \leq s, \quad (2)$$

$$\max_{\mathbf{u}} \mathbf{u}^T \mathbf{A} \mathbf{u} - \rho \|\mathbf{u}\|_0, \quad \text{subject to } \mathbf{u}^T \mathbf{B} \mathbf{u} = 1, \quad (3)$$

for $1 \leq s \leq p$ and $\rho > 0$, where $\|\mathbf{u}\|_0$ is the number of nonzero elements of \mathbf{u} . While Sriperumbudur et al. (2011) only proposed an algorithm to solve a variant of (3), Song

et al. (2015) later proposed several approximate solutions of (3). Recently, Tan et al. (2016) proposed to solve (2), by truncating the steepest ascent iterates in maximizing the Rayleigh coefficient $\mathbf{u} \mapsto \mathbf{u}^T \mathbf{A} \mathbf{u} / \mathbf{u}^T \mathbf{B} \mathbf{u}$. Gaynanova et al. (2017) pointed out a fundamental difference between the penalized and constrained optimizations for sparse GEP, similar to (2) and (3) but with ℓ_1 -norm. Safo et al. (2018) proposed to estimate \mathbf{u} via minimizing $\|\mathbf{u}\|_1$ subject to a constraint $\|\mathbf{A}\tilde{\mathbf{u}} - \tilde{\lambda}\mathbf{B}\tilde{\mathbf{u}}\|_\infty \leq \rho$, where $(\tilde{\lambda}, \tilde{\mathbf{u}})$ is the non-sparse solution of (1). As it is evident in Sriperumbudur et al. (2011), Song et al. (2015), and Tan et al. (2016) who limit themselves for solving only one eigen-pair, we are unclear how (2) or (3) generalizes to simultaneously solving for multiple eigenvectors, $\mathbf{u}_1, \dots, \mathbf{u}_d$. When multiple eigenvectors are needed, as is typical in practice, these methods are not readily applicable, at least not without a clever modification. Our algorithm is designed to estimate $\mathbf{u}_1, \dots, \mathbf{u}_d$ altogether, and works well when $d > 1$.

Han and Clemmensen (2016) assumed \mathbf{B} to be positive definite, and transformed the GEP to a regular eigen-decomposition of $\mathbf{B}^{-1}\mathbf{A}$ (or $\mathbf{B}^{-1/2}\mathbf{A}\mathbf{B}^{-1/2}$) while applying an ℓ_1 -penalty to achieve sparsity. However, their method is not directly applicable to the large- p -small- n -case, due to the numerically unstable inverse of the large matrix \mathbf{B} . They used alternating direction method of multipliers for optimization, which causes their method to be computationally expensive.

Chen et al. (2010) proposed to solve sufficient dimension reduction (SDR) problems by maximizing $\text{trace}(\mathbf{U}^T \mathbf{A} \mathbf{U}) - \rho_\lambda(\mathbf{U})$, for $\mathbf{U} \in \mathbb{R}^{p \times d}$ satisfying $\mathbf{U}^T \mathbf{B} \mathbf{U} = \mathbf{I}_d$, in which the penalty function ρ_λ enforces coordinate-wise sparsity (10). While Chen et al. (2010)'s formulation is similar to our Fast POI with (10), their computation is much slower than any of our proposed algorithms, perhaps due to using both penalization and constraint.

Our proposed algorithms provide sparse solutions of the original GEP (1), produces any number of eigenpairs simultaneously, is computationally efficient even for high-dimensional data, and is applicable to a number of statistical problems including PCA, LDA, CCA, SDR and invariant co-ordinate selection.

The rest of the paper is organized as follows. In Section 2, we introduce the proposed sparse GEP methodology. Numerical algorithms are discussed in Section 3. We demonstrate applications of our proposal to a number of statistical problems including PCA,

LDA, SDR and CCA in Section 4, in which some of the most promising competitors are numerically compared. All proofs are contained in the appendix. The online supplementary material contains additional numerical results.

2 Methodology

2.1 Setting

In most applications, the population matrices \mathbf{A} and \mathbf{B} in (1) are symmetric non-negative definite, while \mathbf{B} is often positive definite. For some applications, the rank of \mathbf{A} is much smaller than the dimension p of the matrices.

We are interested in estimating the generalized eigenvectors $\mathbf{u}_1, \dots, \mathbf{u}_d$ corresponding to the d largest generalized eigenvalues, where $d \leq \text{rank}(\mathbf{A})$. Our proposed methods estimate the subspace $\mathcal{U}_d = \text{span}(\mathbf{u}_1, \dots, \mathbf{u}_d)$. In order for \mathcal{U}_d to be identifiable, one must assume the following on the size of the eigenvalues:

$$\lambda_1 \geq \dots \geq \lambda_d > \lambda_{d+1} \geq \dots \geq \lambda_p \geq 0.$$

Let $\mathbf{U}_d = [\mathbf{u}_1, \dots, \mathbf{u}_d]$ and $\mathbf{\Lambda}_d = \text{diag}(\lambda_1, \dots, \lambda_d)$. The generalized eigenvectors are \mathbf{B} -orthogonal, and thus in general do not form an orthogonal basis of \mathcal{U}_d . However, one can readily obtain an orthogonal basis of \mathcal{U}_d from \mathbf{U}_d , and, conversely, obtain \mathbf{U}_d from any orthogonal basis of \mathcal{U}_d . The detail follows. Throughout the paper, the notation $\mathcal{O}(p, d)$ is used for the set of semi-orthogonal matrices; $\mathcal{O}(p, d) = \{\mathbf{X} \in \mathbb{R}^{p \times d} : \mathbf{X}^T \mathbf{X} = \mathbf{I}_d\}$. Let $\mathcal{O}(d) = \mathcal{O}(d, d)$ be the set of $d \times d$ orthogonal matrices.

The following equation is equivalent to (1):

$$\mathbf{A}\mathbf{U}_d = \mathbf{B}\mathbf{U}_d\mathbf{\Lambda}_d. \tag{4}$$

By the QR decomposition, we have $\mathbf{U}_d = \mathbf{Q}_d\mathbf{R}_d$, for a $\mathbf{Q}_d \in \mathcal{O}(p, d)$, and for a $d \times d$ upper-triangular matrix \mathbf{R}_d . Then the GEP in (4) is equivalently written as

$$\mathbf{A}\mathbf{Q}_d = \mathbf{B}\mathbf{Q}_d\mathbf{\Lambda}_d^*, \tag{5}$$

where $\mathbf{\Lambda}_d^* = \mathbf{R}_d\mathbf{\Lambda}_d\mathbf{R}_d^{-1}$ is a $d \times d$ upper-triangular matrix. Note that the diagonal elements of $\mathbf{\Lambda}_d^*$ are the same as those of $\mathbf{\Lambda}_d$.

Now suppose we have an arbitrary basis matrix $\tilde{\mathbf{Q}}_d \in \mathcal{O}(p, d)$ such that $\text{span}(\tilde{\mathbf{Q}}_d) = \mathcal{U}_d$. The generalized eigenvectors satisfying (4) can be recovered, as follows:

Proposition 1. *Assume that $\tilde{\mathbf{Q}}_d$ is an arbitrary $p \times d$ orthogonal matrix with the same column space as \mathbf{U}_d , where $(\mathbf{\Lambda}_d, \mathbf{U}_d)$ is the solution to (4). For $\tilde{\mathbf{A}}_d = \tilde{\mathbf{Q}}_d^T \mathbf{A} \tilde{\mathbf{Q}}_d$ and $\tilde{\mathbf{B}}_d = \tilde{\mathbf{Q}}_d^T \mathbf{B} \tilde{\mathbf{Q}}_d$, let \mathbf{T} and \mathbf{D} respectively be the matrix of eigenvectors and the diagonal matrix of eigenvalues of the following GEP:*

$$\tilde{\mathbf{A}}_d \mathbf{T} = \tilde{\mathbf{B}}_d \mathbf{T} \mathbf{D} \tag{6}$$

with $\mathbf{T}^T \tilde{\mathbf{B}}_d \mathbf{T} = \mathbf{I}_d$. Then $\text{span}(\mathbf{U}_d) = \text{span}(\tilde{\mathbf{Q}}_d \mathbf{T})$. If the diagonal values of \mathbf{D} are distinct and in the decreasing order, then $\mathbf{U}_d = \tilde{\mathbf{Q}}_d \mathbf{T}$ and $\mathbf{\Lambda}_d = \mathbf{D}$.

In the next subsection, we discuss our approaches in estimating an orthogonal basis of \mathcal{U}_d , i.e., \mathbf{Q}_d in (5), from noisy versions of \mathbf{A} and \mathbf{B} . Proposition 1 can then be used to obtain the estimates of the generalized eigenvector and eigenvalue pair $(\mathbf{U}_d, \mathbf{\Lambda}_d)$. In practice the matrices \mathbf{A} and \mathbf{B} in (4) are replaced by their empirical counterparts computed from a sample. We treat \mathbf{A} and \mathbf{B} to be the empirical matrices, with which we attempt to solve the GEP. In most applications, the empirical matrices \mathbf{A} and \mathbf{B} are non-negative definite by construction. We require \mathbf{B} to be positive definite. If not, we add a scaled identity matrix $\epsilon \mathbf{I}_p$, for a small $\epsilon > 0$, and $\mathbf{B} + \epsilon \mathbf{I}_p$ is treated as \mathbf{B} . We recommend using $\epsilon = \min(\log p / \text{rank}(\mathbf{B}), \sigma_{\mathbf{B}}/2)$ where the $\sigma_{\mathbf{B}}$ is the smallest positive eigenvalue of \mathbf{B} .

2.2 Proposed Method

We consider two penalized optimization approaches in order to obtain sparse solutions of the GEP. The first approach is a generalization of the widely used orthogonal iteration and can be applied to almost all situations. The second approach aims to provide efficient computation for some high-dimensional problems, such as PCA and multiclass LDA.

2.2.1 Penalized Orthogonal Iteration

We begin by reviewing the standard generalized orthogonal iteration in solving the GEP (5). Given (\mathbf{A}, \mathbf{B}) and an initial value $\hat{\mathbf{Q}}_0 \in \mathcal{O}(p, d)$, the standard generalized orthogonal

iteration (Section 8.7.3, Golub and Van Loan, 1996) finds $\hat{\mathbf{Q}}$, a solution of (5), by iterating the following two steps until convergence. For $r = 1, 2, \dots$,

Step 1. Solve $\mathbf{B}\hat{\mathbf{Z}}_r = \mathbf{A}\hat{\mathbf{Q}}_{r-1}$ for $\hat{\mathbf{Z}}_r$.

Step 2. Obtain $\hat{\mathbf{Q}}_r$ by QR decomposition $\hat{\mathbf{Z}}_r = \hat{\mathbf{Q}}_r\hat{\mathbf{R}}_r$.

The iteration stops when a distance between $\hat{\mathbf{Q}}_{r-1}$ and $\hat{\mathbf{Q}}_r$ is smaller than a threshold.

We use the projection distance between the subspaces, defined later in (22).

The penalized orthogonal iteration (POI) modifies Step 1 so that it can be cast into a convex optimization framework with a sparsity-inducing penalty. Let $p_\lambda(\mathbf{Z})$ be a penalty function on the matrix \mathbf{Z} . Here, $\lambda \geq 0$ represents the degrees of penalization, yielding $p_\lambda(\mathbf{Z}) = 0$ if $\lambda = 0$. We propose to replace Step 1 by

$$\hat{\mathbf{Z}}_r = \operatorname{argmin}_{\mathbf{Z} \in \mathbb{R}^{p \times d}} \left\{ \operatorname{trace} \left(\frac{1}{2} \mathbf{Z}^T \mathbf{B} \mathbf{Z} - \mathbf{Z}^T \mathbf{A} \hat{\mathbf{Q}}_{r-1} \right) + p_\lambda(\mathbf{Z}) \right\}. \quad (7)$$

Note that if $\lambda = 0$, then $\hat{\mathbf{Z}}_r$ of (7) is the solution of the original equation:

$$\mathbf{B}\hat{\mathbf{Z}}_r = \mathbf{A}\hat{\mathbf{Q}}_{r-1}. \quad (8)$$

The POI optimization problem (7) is motivated by the fact that the linear equation system (8) is the first-order condition of a quadratic optimization problem (7) without the penalty term.

A natural choice for the sparsity-inducing penalty function $p_\lambda(\mathbf{Z})$ in (7) is a lasso penalty (Tibshirani, 1996),

$$p_\lambda(\mathbf{Z}) = \sum_{j=1}^d \lambda_j \|\mathbf{z}_j\|_1, \quad (9)$$

where $\mathbf{Z} = [\mathbf{z}_1, \dots, \mathbf{z}_d]$ and $\lambda_j > 0$. While (9) generally produces *element-wise sparse* solutions, it may be more reasonable to assume that there exists a small subset of coordinate indices that are relevant to all of the d largest generalized eigenvalues. For this purpose, we use the $\ell_{2,1}$ -norm penalty for $p_\lambda(\mathbf{Z})$, also known as the group-lasso penalty (Yuan and Lin, 2006). Let \mathbf{z}_i^T be the i th row of \mathbf{Z} ($i = 1, \dots, p$). Then we set for $\lambda > 0$,

$$p_\lambda(\mathbf{Z}) = \lambda \sum_{i=1}^p \|\mathbf{z}_i\|_2. \quad (10)$$

We have implemented the POI with the penalty (9) for element-wise sparsity and (10) for *coordinate-wise sparsity*. Other choices of penalty functions can be used as well; see, for example, Tibshirani (2011).

In search of a sparse subspace basis, coordinate-wise sparsity is preferred to element-wise sparsity, since any element-wise sparse basis matrix \mathbf{Q} is in general no longer element-wise sparse if arbitrarily rotated, e.g., in the orthogonalization step of the POI. In contrast, $\mathbf{Q}\mathbf{V}$ for any $\mathbf{V} \in \mathcal{O}(d)$ is coordinate-wise sparse as long as \mathbf{Q} is coordinate-wise sparse. Since the basis of a subspace can only be coordinate-wise sparse, utilizing the coordinate-wise sparsity has a clear advantage in variable selection and its interpretation (*cf.* Bouveyron et al., 2016).

Remark 1. In the PCA context (i.e, $\mathbf{B} = \mathbf{I}_p$ and $\mathbf{A} = \widehat{\Sigma}$, the sample covariance matrix), the POI overlaps with the sparse PCA algorithm of Ma (2013), who proposed to add a thresholding step to the orthogonal iteration for the standard eigenvalue problem. In particular, if the penalty function p_λ is given by an ℓ_1 -norm, then our method coincides with Ma’s method with soft-thresholding.

2.2.2 Fast POI

A computationally simpler alternative to the POI is to solve an alternative form of (7) just once. For this, we propose to replace $\mathbf{A}\mathbf{Q}_{r-1}$ in (7) with the $p \times d$ matrix, denoted by \mathbf{V} , whose columns contain the eigenvectors of \mathbf{A} that correspond to the d largest eigenvalues of \mathbf{A} . This results in the following:

$$\hat{\mathbf{Z}} = \operatorname{argmin}_{\mathbf{Z} \in \mathbb{R}^{p \times d}} \left\{ \operatorname{trace} \left(\frac{1}{2} \mathbf{Z}^T \mathbf{B} \mathbf{Z} - \mathbf{Z}^T \mathbf{V} \right) + p_\lambda(\mathbf{Z}) \right\}. \quad (11)$$

The orthogonal basis matrix $\hat{\mathbf{Q}}$ is obtained by the QR decomposition of $\hat{\mathbf{Z}}$. There is no “outer” iteration for this approach, which yields much faster computation. The penalty function $p_\lambda(\mathbf{Z})$ can be chosen to be either (9) or (10). The solutions from this approach is referred to as *Fast POI* solutions.

Note that the POI solves the GEP in (5) if $\lambda = 0$. On the other hand, the Fast POI solution with $\lambda = 0$ does not in general solve the original GEP. The following proposition identifies a sufficient condition under which the Fast POI solution with no penalty solves the original GEP.

Proposition 2. *Suppose \mathbf{A} and \mathbf{B} are both $p \times p$ symmetric non-negative matrices. For any $1 \leq d < p$, let $\mathbf{V} \in \mathcal{O}(p, d)$ be the eigenvector-matrix of \mathbf{A} corresponding to the d*

largest eigenvalues of \mathbf{A} , and $\mathbf{Q} \in \mathcal{O}(p, d)$ satisfy the generalized eigen-equation (5). If

(a) $\mathbf{B} = \mathbf{I}_p$, or

(b) \mathbf{B} is positive definite and $\text{rank}(\mathbf{A}) = d$,

then the column space of $\mathbf{B}^{-1}\mathbf{V}$ is exactly the column space of \mathbf{Q} .

The condition (a) corresponds to the standard eigenvalue problem, arising in the context of PCA. The rank condition in (b) is satisfied when there are $K = d+1$ groups in a multiclass LDA problem.

In our experience, obtaining a Fast POI solution requires only a fraction of time that is needed for the corresponding POI solution. This is because POI typically requires many iterations until convergence. Despite its quick computing time, we found that Fast POI in the problems of PCA and multiclass LDA provides good approximations of the POI solutions.

Remark 2. After we formulated the Fast POI criterion, we found that, in the special case of multiclass LDA problems, our minimization approach (11) is similar to the sparse LDA methods of Mai et al. (2017) and Gaynanova et al. (2016). Using the notation used in (11), Mai et al’s solutions are given by replacing \mathbf{V} with the mean difference matrix with columns $\hat{\mu}_k - \hat{\mu}_1$, $k = 2, \dots, K$; Gaynanova et al’s approach is equivalent to (11) if $-\mathbf{Z}^T\mathbf{V}$ is replaced by $\frac{1}{2}\mathbf{Z}^T\mathbf{AZ} - \mathbf{Z}^T\mathbf{D}$, where \mathbf{D} consists of weighted mean differences $\hat{\mu}_i - \hat{\mu}_j$. Both approaches are dependent on the order of group labels and, consequently, their solutions change if different label orders are used. In Gaynanova et al’s approach, the inclusion of $\frac{1}{2}\mathbf{Z}^T\mathbf{AZ}$ is to ensure the objective function to be bounded below. Since we use $\mathbf{B} + \epsilon\mathbf{I}_p$ (if \mathbf{B} is not full rank), the objective function (11) is bounded. These methods are further compared numerically in Section 4.2.

2.3 Eigenvalue Estimation

Once $\hat{\mathbf{Q}}$ is obtained either by POI or Fast POI, one might be interested in estimating the corresponding generalized eigenvalues. We illustrate two approaches here. First, one can estimate the generalized eigenvalues by directly using Proposition 1. Let $\hat{\mathbf{T}}$ and $\hat{\mathbf{D}}$

be the solution to the GEP (6) with \mathbf{Q} replaced by $\hat{\mathbf{Q}}$. Then the plug-in estimate of the eigenvector matrix is $\hat{\mathbf{U}} = \hat{\mathbf{Q}}\hat{\mathbf{T}}$, and the eigenvalue matrix estimate is $\hat{\mathbf{\Lambda}} = \hat{\mathbf{D}}$. If the elements of \mathbf{A} stand for covariances, then using Proposition 1 is equivalent to estimating λ_j by the empirical variance contained in \mathbf{A} projected on $\hat{\mathbf{u}}_j$, normalized by that of \mathbf{B} :

$$\hat{\lambda}_j = \hat{\mathbf{u}}_j^T \mathbf{A} \hat{\mathbf{u}}_j / \hat{\mathbf{u}}_j^T \mathbf{B} \hat{\mathbf{u}}_j, \quad j = 1, \dots, d. \quad (12)$$

A more sophisticated approach is to use the eigen-equation (4) directly. For this, we estimate the generalized eigenvalue matrix $\mathbf{\Lambda}$ by the solution of the following minimization problem:

$$\tilde{\mathbf{\Lambda}} = \underset{\mathbf{\Lambda}}{\operatorname{argmin}} \left\| \mathbf{A}\hat{\mathbf{U}} - \mathbf{B}\hat{\mathbf{U}}\mathbf{\Lambda} \right\|_F^2, \quad (\mathbf{\Lambda} \text{ is diagonal}). \quad (13)$$

This problem has a closed-form solution.

Lemma 3. *Let $\boldsymbol{\alpha}_j$ and $\boldsymbol{\beta}_j$ be the j th column vectors of $\mathbf{A}\hat{\mathbf{U}}$ and $\mathbf{B}\hat{\mathbf{U}}$. Then the solution $\tilde{\mathbf{\Lambda}}$ of (13) is $\tilde{\mathbf{\Lambda}} = \operatorname{diag}(\tilde{\lambda}_1, \dots, \tilde{\lambda}_d)$, where $\tilde{\lambda}_j = (\boldsymbol{\beta}_j^T \boldsymbol{\beta}_j)^{-1} \boldsymbol{\beta}_j^T \boldsymbol{\alpha}_j$.*

The eigenvalue estimates $\hat{\mathbf{\Lambda}}$ of (12) and $\tilde{\mathbf{\Lambda}}$ of (13) are in general different. They are the same when $\hat{\mathbf{u}}_j$ are the exact solutions of the GEP (4), which are generally non-sparse. In our experiments, these two estimates were numerically close to each other. We used (12) in all of our numerical analyses.

2.4 Tuning Parameter Selection

The tuning parameter λ in the penalty function plays an important role in the estimation. When $\lambda = 0$, our proposal provides non-sparse solutions, while the estimated subspaces tend to have more sparse bases as λ increases. We consider a general cross-validation approach that can be used for any regularized GEP.

Suppose that we have a data set that can be split into two subsets that produce independent pairs $(\mathbf{A}^{(r)}, \mathbf{B}^{(r)})$, $r = 1, 2$. We use the data indexed by $r = 1$ to train the estimates $\hat{\mathbf{U}}_\lambda$ and $\hat{\mathbf{\Lambda}}_\lambda$ for various values of λ . The data indexed by $r = 2$ is used to evaluate these estimates, to tune λ . In particular, for a given λ , we define the cross-validation score as

$$CV(\lambda) = \operatorname{trace} \left[(\hat{\mathbf{U}}_\lambda^T \mathbf{B}^{(2)} \hat{\mathbf{U}}_\lambda)^{-1} \hat{\mathbf{U}}_\lambda^T \mathbf{A}^{(2)} \hat{\mathbf{U}}_\lambda \right]. \quad (14)$$

We choose the λ with the largest average cross-validation score, based on repeated random splits, or by predefining the training and tuning sets. Candidate values of λ are found in an interval $(0, \lambda_{\max})$.

The upper bound λ_{\max} is set so that $\hat{\mathbf{U}}_\lambda = \mathbf{0}$ for any $\lambda > \lambda_{\max}$, and depends on the data and the penalty term used. We defer the discussion on the choice of λ_{\max} to Section 3; see Remarks 3 and 4.

We interpret the CV score (14) as follows. Note that when $\mathbf{B}^{(2)}$ and $\mathbf{A}^{(2)}$ are replaced by $\mathbf{B}^{(1)}$ and $\mathbf{A}^{(1)}$, $CV(\lambda)$ is simply the sum of estimated eigenvalues (12). Heuristically, maximizing $CV(\lambda)$ is equivalent to finding the subspace with the largest sum of “prediction eigenvalues”. We delve further into the following data-analytic situations.

For PCA, $CV(\lambda)$ represents the total variance contained in the d -dimensional eigenspace. To be specific, let \mathbf{X} be the centered $n \times p$ data matrix, then we set $\mathbf{A}^{(2)} = \mathbf{X}^T \mathbf{X}$ and $\mathbf{B}^{(2)} = \mathbf{I}_p$, which in turn leads to

$$CV(\lambda) = \text{trace}(\hat{\mathbf{U}}_\lambda^T \mathbf{A}^{(2)} \hat{\mathbf{U}}_\lambda) = \text{trace}(\mathbf{X}^T \mathbf{X}) - \|\mathbf{X}(\mathbf{I}_p - \hat{\mathbf{U}}_\lambda \hat{\mathbf{U}}_\lambda^T)\|_F^2,$$

where the second term is sometimes called *the reconstruction error* of the subspace spanned by $\hat{\mathbf{U}}_\lambda$. Thus maximizing $CV(\lambda)$ is equivalent to minimizing the reconstruction error, an approach that can be found in the literature on PCA; see e.g., Shen and Huang (2008); Josse and Husson (2012). In our numerical studies, we found that $CV(\lambda)$ is typically a concave function, and is negatively correlated with the distance to the true eigenspace from the estimate associated with λ , i.e. the larger $CV(\lambda)$, the better the estimation. These are illustrated in Fig. 1 (top two panels) with simulated data, further discussed in Section 4.

In a situation with multiple groups (*cf.* Section 4.2), we set $\mathbf{A}^{(2)} = \mathbf{S}_B$ as the between-group covariance, and $\mathbf{B}^{(2)} = \mathbf{S}_W$ as the within-group covariance, estimated from the tuning set. The groups are more clearly separated for larger \mathbf{S}_B and smaller \mathbf{S}_W . Thus, $CV(\lambda)$ is large if the groups, projected on the subspace spanned by $\hat{\mathbf{U}}_\lambda$, are well-separated. In a view from clustering, $CV(\lambda)$ is akin to the so-called CH index (Caliński and Harabasz, 1974) in spirit; they are proportional to each other if $d = 1$. Larger CH index indicates clearer clustering, which is also associated with larger $CV(\lambda)$. Figure 1 (bottom three panels) shows that, in the case of multiclass LDA, $CV(\lambda)$ is a concave function of λ and is negatively correlated with the misclassification rate. This is not unexpected, because

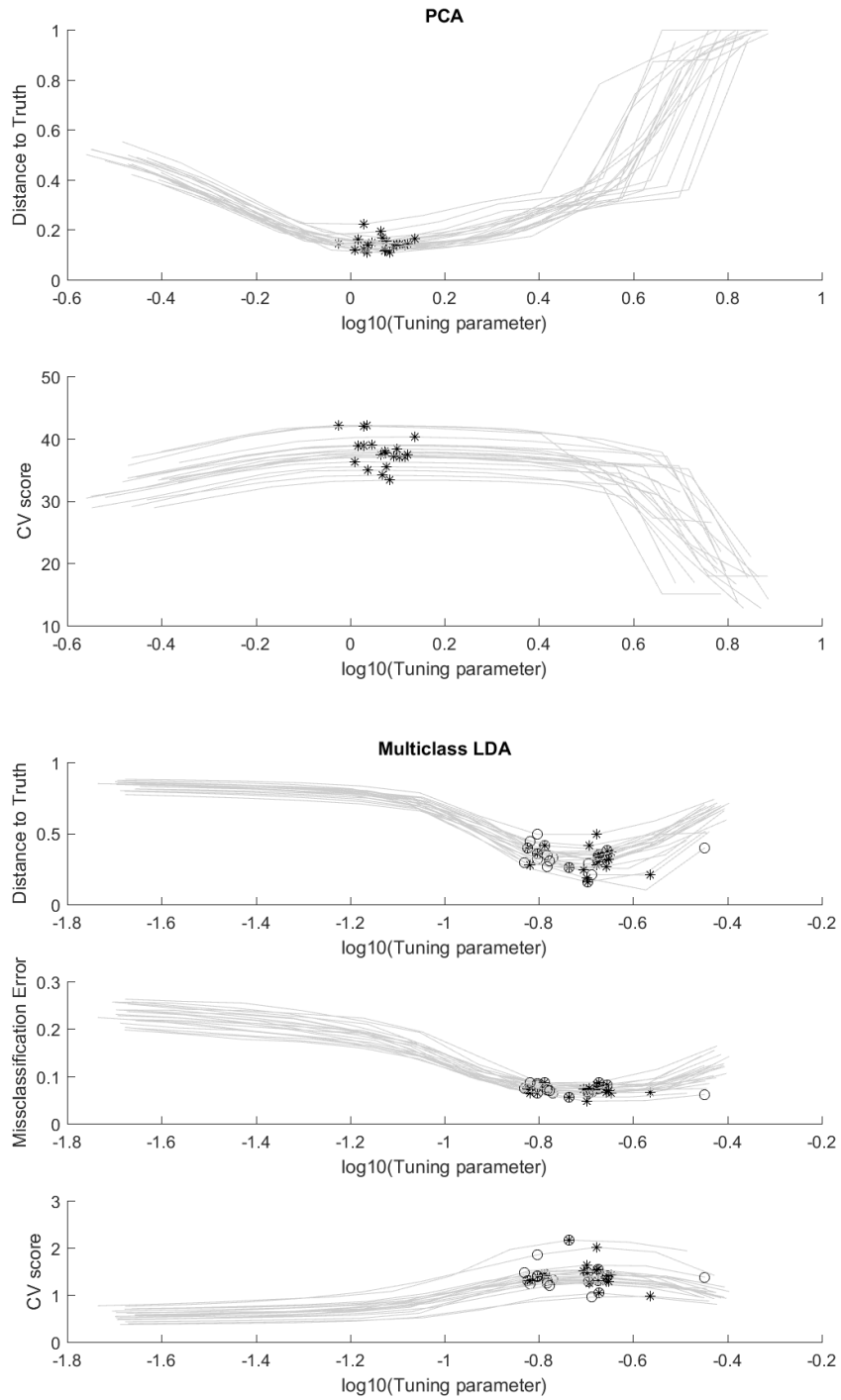


Figure 1: The proposed tuning procedure works well for our simulated data. Top two panels are from PCA models; bottom three panels are from multiclass LDA models. * indicates the location of tuned λ that maximizes $CV(\lambda)$. \circ indicates the location of tuned λ that minimizes the tuning misclassification error rate.

larger $CV(\lambda)$ implies clearer separation of groups, which in turn makes the classification easier.

For classification in mind, one may use the misclassification rate as a tuning criterion. Tuning by (14) is in fact on par with tuning by misclassification rate; see Section 4.2. The tuned λ by both methods are close to each other, as shown in Fig. 1.

We note that since our tuning procedure is intended for eigenspace prediction accuracy, it sometimes chooses more variables than desired. For more precise variable selection, one may adopt the one-standard error rule; choose the most parsimonious model within one standard error of the maximum $CV(\lambda)$, which may only be estimated under multiple splits of data as in K -fold cross-validation.

3 Algorithms

The POI and Fast POI solutions can be efficiently implemented. We provide algorithms to solve the POI (7) when the penalty function is either (9) or (10). Note that the Fast POI (11) can be solved in the same way (7) is solved, with $\mathbf{A}\mathbf{Q}_{r-1}$ replaced by \mathbf{V} . Our algorithms for (7) are guaranteed to converge to the optimal solution (*cf.* Tseng, 1993), thus the Fast POI always converges. We are not aware of a general condition under which the proposed POI is guaranteed to converge, although it has converged in all of our experiments.

3.1 Algorithm for element-wise sparse estimation

Solving (7) with the penalty (9) amounts to solving d separate problems. Specifically, the j th column \mathbf{z}_j of \mathbf{Z}_r is

$$\mathbf{z}_j = \operatorname{argmin}_{\mathbf{z} \in \mathbb{R}^p} \left\{ \left(\frac{1}{2} \mathbf{z}^T \mathbf{B} \mathbf{z} - \mathbf{z}^T \mathbf{A} \mathbf{q}_j \right) + \lambda_j \|\mathbf{z}\|_1 \right\}, \quad (15)$$

where \mathbf{q}_j is the j th column of \mathbf{Q}_{r-1} . The minimization problem (15) can be efficiently solved by the cyclic coordinate descent algorithm. The algorithm updates the coordinates of the iterate \mathbf{z} in a cyclic fashion. In particular, let $S_\lambda(z) = \operatorname{sign}(z)(|z| - \lambda)_+$ be the soft-thresholding operator. Then, the i th coordinate z_i of \mathbf{z} is updated by

$$z_i \leftarrow S_{\lambda_j} (\mathbf{a}_i^T \mathbf{q}_j - \mathbf{b}_i^T \mathbf{z} + b_{ii} z_i) / b_{ii}, \quad (16)$$

where b_{ii} is the i th diagonal element of \mathbf{B} , and \mathbf{a}_i^T (or \mathbf{b}_i^T) is the i th row of the symmetric matrix \mathbf{A} (or \mathbf{B} , respectively).

Remark 3. For both POI and Fast POI, setting too large λ_j gives the trivial solution $\mathbf{z}_j = 0$. It can be shown that $\lambda_j^o = \max_{i=1,\dots,p} |\mathbf{a}_i^T \mathbf{q}_j|$ is the maximum value of λ_j which gives a non-trivial solution of (15). However, λ_j^o depends on the iterate $\hat{\mathbf{Q}}_{r-1}$. Since the solution \mathbf{z}_j of (15) is sparse for large λ_j , we take the maximum of λ_j^o over the possible values of “sparse” $\mathbf{Q}_{r-1} \in \mathcal{O}(p, d)$ such that each column of \mathbf{Q}_{r-1} has only one nonzero entry. For $\mathcal{O}_0(p, d) = \{\mathbf{Q} \in \mathcal{O}(p, d) : \#\{(i, j) : q_{ij} \neq 0\} = d\}$, we set

$$\lambda_{\max} = \max_{i=1,\dots,p} \left\{ \max_{\mathbf{Q} \in \mathcal{O}_0(p,d)} \max_{j=1,\dots,d} |\mathbf{a}_i^T \mathbf{q}_j| \right\} = \max_{i,j} |a_{ij}|, \quad (17)$$

where a_{ij} is the (i, j) th element of \mathbf{A} .

3.2 Algorithm for coordinate-wise sparse estimation

Since the problem (7) is convex and the penalty function (10) is block-separable, the block coordinate descent algorithm is guaranteed to converge to an optimal solution (Tseng, 1993). Denote \mathbf{q}_j and \mathbf{q}_i^T for the j th column and i th row of \mathbf{Q}_{r-1} , respectively. Define $\mathbf{z}_o^T = [\mathbf{z}_1^T, \dots, \mathbf{z}_d^T]$ and $\mathbf{q}_o^T = [\mathbf{q}_1^T, \dots, \mathbf{q}_d^T]$, $\mathbf{z}^T = [\mathbf{z}_1^T, \dots, \mathbf{z}_p^T]$ and $\mathbf{q}^T = [\mathbf{q}_1^T, \dots, \mathbf{q}_p^T]$. Then,

$$\begin{aligned} \text{trace} \left(\frac{1}{2} \mathbf{Z}^T \mathbf{B} \mathbf{Z} - \mathbf{Z}^T \mathbf{A} \mathbf{Q}_{r-1} \right) &= \sum_{j=1}^d \left(\frac{1}{2} \mathbf{z}_j^T \mathbf{B} \mathbf{z}_j - \mathbf{z}_j^T \mathbf{A} \mathbf{q}_j \right) \\ &= \frac{1}{2} \mathbf{z}_o^T (\mathbf{I}_d \otimes \mathbf{B}) \mathbf{z}_o - \mathbf{z}_o^T (\mathbf{I}_d \otimes \mathbf{A}) \mathbf{q}_o \\ &= \frac{1}{2} \mathbf{z}^T (\mathbf{B} \otimes \mathbf{I}_d) \mathbf{z} - \mathbf{z}^T (\mathbf{A} \otimes \mathbf{I}_d) \mathbf{q} \\ &= \frac{1}{2} \sum_{i=1}^p \sum_{j=1}^p \mathbf{z}_i^T b_{ij} \mathbf{z}_j - \sum_{i=1}^p \mathbf{z}_i^T \boldsymbol{\delta}_i, \end{aligned} \quad (18)$$

where a_{ij} , (or b_{ij}) is the (i, j) th element of \mathbf{A} (or \mathbf{B} , respectively) and $\boldsymbol{\delta}_i = \sum_{j=1}^p a_{ij} \mathbf{q}_j$. Using the fact that \mathbf{B} is symmetric, for the g th block with all \mathbf{z}_i , $i \neq g$, fixed, the problem becomes

$$\min_{\mathbf{z}_g} \left\{ \frac{1}{2} \mathbf{z}_g^T b_{gg} \mathbf{z}_g - \mathbf{z}_g^T \mathbf{a}_g + \lambda \|\mathbf{z}_g\|_2 \right\}, \quad (19)$$

where $\mathbf{a}_g = \boldsymbol{\delta}_g - \sum_{i \neq g} b_{gi} \mathbf{z}_i$, and its solution is obtained by

$$\hat{\mathbf{z}}_g = \frac{1}{b_{gg}} \left(1 - \frac{\lambda}{\|\mathbf{a}_g\|_2} \right)_+ \mathbf{a}_g. \quad (20)$$

In short, the algorithm updates \mathbf{Z} in a cyclic fashion, with the initial value given by $\mathbf{Z} = \mathbf{Q}_{r-1}$. For $g = 1, \dots, p$, the g th row \mathbf{z}_g^\top of \mathbf{Z} is updated by (20) until a convergence criterion is met.

Remark 4. It is easy to see that $\lambda_0 = \max_{g=1, \dots, p} \|\boldsymbol{\delta}_g\|_2$ is the maximum value of λ that gives a non-trivial solution of (19). Since $\boldsymbol{\delta}_g = \sum_{j=1}^p a_{gj} \mathbf{q}_j$ depends on the iterate \mathbf{Q}_{r-1} of the POI, we take

$$\lambda_{\max} = \max_{g=1, \dots, p} \left\{ \max_{\mathbf{Q} \in \mathcal{O}_0(p, d)} \left\| \sum_{j=1}^p a_{gj} \mathbf{q}_j \right\|_2 \right\}, \quad (21)$$

which provides an *upper bound* for the maximum value of λ . Note that in (21) we used $\mathbf{Q} \in \mathcal{O}_0(p, d)$ whose entrywise L_0 -norm is d (that is, as sparse as possible). To simplify (21), for each fixed g , denote $a_{g,(j)}$ for the j th largest element among the g th row of \mathbf{A} , in the absolute value. Then $\max_{\mathbf{Q} \in \mathcal{O}_0(p, d)} \left\| \sum_{j=1}^p a_{gj} \mathbf{q}_j \right\|_2 = (\sum_{j=1}^d a_{g,(j)}^2)^{1/2}$, which in turn gives, for POI solutions,

$$\lambda_{\max} = \max_{g=1, \dots, p} \left(\sum_{j=1}^d a_{g,(j)}^2 \right)^{1/2}.$$

For an upper bound of the tuning parameter used in Fast POI, it is straightforward to see that $\lambda_{\max} = \max_{g=1, \dots, p} (\sum_{j=1}^d v_{gj}^2)^{1/2}$, where v_{gj} is the (g, j) th element of \mathbf{V} .

4 Applications to Multivariate Analysis

In this section, we demonstrate the application of the proposed algorithms to principal component analysis (PCA), multiclass linear discriminant analysis (LDA), sufficient dimension reduction (SDR) and canonical correlation analysis (CCA).

4.1 Sparse Principal Component Analysis

The standard PCA amounts to solving the ordinary eigen-decomposition of the covariance matrix $\boldsymbol{\Sigma}$. By setting $\mathbf{A} = \boldsymbol{\Sigma}$, $\mathbf{B} = \mathbf{I}_p$, the problem (1) becomes the ordinary eigen-decomposition problem, and the solution $(\mathbf{u}_j, \lambda_j)$ corresponds to the principal component (PC) direction and variance pair.

We demonstrate the application of our method to sparse PCA, using a large-scale genomic data. The data set we use is adopted from Ciriello et al. (2015), and consists of

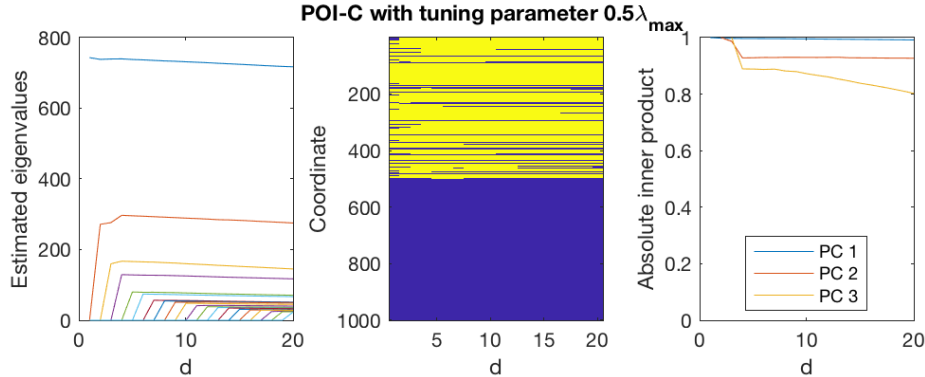


Figure 2: Sparse PCA by POI with coordinate-wise sparse penalty for a genomic data set. The analysis is repeated for subspace dimension $d = 1$ to 20. Shown are estimated eigenvalues (left), nonzero coordinates shown as lighter color (middle) and $|\hat{\mathbf{q}}_{i,i}^T \hat{\mathbf{q}}_{i,d}|$ for $i = 1, 2, 3$, where $\hat{\mathbf{q}}_{i,d}$ is the i th PC direction estimate when estimating PC subspace of dimension d (right).

272 cases of 1000 variables, where the first 500 variables are gene expression levels from the original data set, and the latter 500 are normally distributed random noises. Since it is typical that in performing PCA one does not know which dimension d to choose, we explore $d = 1$ to 20, and estimate the principal subspace of dimension d using POI with coordinate-wise sparse penalty. A graphical summary of this study can be found in Fig. 2. It can be seen that the eigenvalue and eigenvector estimates are stable across different choices of d , and our method has correctly screened out the noise variables for all choices of d . See the online supplementary material for details.

We now present a simulation study to compare the performance of our application to sparse PCA with competing methods (Zou et al., 2006; Shen and Huang, 2008; Song et al., 2015). We simulate from p -variate normal distribution with mean zero and covariance matrix Σ . Let d stand for the number of distinguishable principal components. We use $d = 3$ or 5. Let $\Sigma = \mathbf{U}_d \Lambda_d \mathbf{U}_d^T + \mathbf{I}_p$, where Λ_d is the diagonal matrix consisting of eigenvalues, satisfying $\text{diag}(\Lambda_d^{1/2}) = 3(5, 4, \dots, 5 - d + 1)$. We use three models for the $p \times d$ eigenvector matrix \mathbf{U}_d , defined below.

Model I: The eigenvector matrix \mathbf{U}_d has only $s = 10$ nonzero rows. Specifically, the first s elements in each column of \mathbf{U}_d are $\mathbf{z} / \|\mathbf{z}\|_2$, where \mathbf{z} is independently sampled from $N_s(\mathbf{0}, \mathbf{I}_s)$. The eigenvectors under this model are coordinate-wise sparse.

Model II: For $s = 5$, the first ds rows of \mathbf{U}_d are $s^{-1/2}\mathbf{I}_d \otimes \mathbf{1}_s$, and the rest of rows consist of zeros. Under this model, eigenvectors are not only orthogonal, but also combinations of disjoint sets of coordinates.

Model III: For $s = 5$, the eigenvector matrix \mathbf{U}_d has ds nonzero rows, formed similar to a block-lower-triangular matrix. Specifically, the nonzero rows are given by the QR decomposition of $\mathbf{A}_d \otimes \mathbf{1}_s$, where \mathbf{A}_d is a $d \times d$ lower-triangular matrix, with all lower-triangular elements being one.

Model I calls for a coordinate-wise sparse estimation, Model II for an element-wise sparse estimation, while Model III does not clearly favor any choice of penalty. Both Models II and III seem unnatural to be conceived as a model underlying any real data. As argued in Bouveyron et al. (2016) coordinate-wise sparse principal component directions are more natural to interpret than element-wise sparse directions.

The estimates from our methods are denoted by POI-L, POI-C, FastPOI-L and FastPOI-C, where “L” stands for using the lasso penalty (9), and “C” stands for using the coordinate-wise group lasso penalty (10). For each method, we define a candidate set of tuning parameters $L = \{(0.75)^i \lambda_{\max} : i = 0, 1, \dots, t, \infty\}$. We set $t = 31$, and λ_{\max} as the upper bound for L as defined in Remarks 3 and 4. For each choice of $\lambda \in L$, we compute the cross-validation score (14), using an independent tuning set of data.

The performance of each method is measured by a distance between the estimated subspace, spanned by $\widehat{\mathbf{U}}_d$, and the true eigenspace \mathbf{U}_d . The principal angles θ_i between two subspaces are often used to measure the distance. The principal angles between $\widehat{\mathbf{U}} \in \mathcal{O}(p, d_1)$ and $\mathbf{U} \in \mathcal{O}(p, d_2)$ are defined as $\theta_i = \arccos(\sigma_i(\widehat{\mathbf{U}}^T \mathbf{U}))$, where $\sigma_i(\mathbf{A})$ is the i th largest singular value of \mathbf{A} . We use the projection metric

$$\rho(\widehat{\mathbf{U}}, \mathbf{U}) = \max\{\sin \theta_i : i = 1, \dots, \min(d_1, d_2)\}. \quad (22)$$

If $d_1 = d_2 = d$, then the projection metric is equivalent to the difference between two corresponding projection matrices: $\rho(\widehat{\mathbf{U}}, \mathbf{U}) = \|\widehat{\mathbf{U}}\widehat{\mathbf{U}}^T - \mathbf{U}\mathbf{U}^T\|$, where $\|\cdot\|$ is the natural spectral norm.

Let $\widehat{\mathbf{U}}(\lambda)$ be the estimate of \mathbf{U} , when tuning parameter λ is used. Denote the cross-validated estimate by $\widehat{\mathbf{U}}(\hat{\lambda})$ where $\hat{\lambda} = \arg \max_{\lambda \in L} CV(\lambda)$. The performances of subspace

| Model | d | p | POI-L | POI-C | FastPOI-L | FastPOI-C | Zou et al. | Song et al. | Shen & Huang |
|-------|-----|-----|--------------|--------------|-----------|--------------|------------|--------------|--------------|
| I | 3 | 200 | 0.196 | 0.159 | 0.200 | 0.162 | 0.195 | 0.252 | 0.196 |
| | 3 | 500 | 0.197 | 0.150 | 0.210 | 0.156 | 0.197 | 0.276 | 0.194 |
| | 5 | 200 | 0.310 | 0.196 | 0.387 | 0.220 | 0.311 | 0.330 | 0.310 |
| | 5 | 500 | 0.348 | 0.204 | 0.450 | 0.363 | 0.303 | 0.448 | 0.343 |
| II | 3 | 200 | 0.106 | 0.162 | 0.155 | 0.160 | 0.124 | 0.104 | 0.105 |
| | 3 | 500 | 0.102 | 0.164 | 0.155 | 0.164 | 0.123 | 0.101 | 0.101 |
| | 5 | 200 | 0.168 | 0.496 | 0.332 | 0.458 | 0.242 | 0.228 | 0.215 |
| | 5 | 500 | 0.169 | 0.561 | 0.397 | 0.699 | 0.290 | 0.308 | 0.207 |
| III | 3 | 200 | 0.108 | 0.150 | 0.177 | 0.154 | 0.151 | 0.105 | 0.106 |
| | 3 | 500 | 0.117 | 0.154 | 0.195 | 0.161 | 0.164 | 0.119 | 0.115 |
| | 5 | 200 | 0.214 | 0.343 | 0.479 | 0.404 | 0.400 | 0.371 | 0.294 |
| | 5 | 500 | 0.222 | 0.352 | 0.623 | 0.556 | 0.489 | 0.439 | 0.282 |

Table 1: The minimal projection distance to the truth, averaged from 100 repetitions, for principal subspace estimation. The standard errors are at most 0.023. Smaller distance indicates more precise estimation. Highlighted are the best performed models (within 2 standard error of the smallest).

estimates are measured by the following criteria:

1. The minimal distance to the truth: $\min_{\lambda \in L} \rho(\hat{\mathbf{U}}(\lambda), \mathbf{U})$.
2. The distance from the cross-validated estimate: $\rho(\hat{\mathbf{U}}(\hat{\lambda}), \mathbf{U})$.

For each model we choose the number of principal components as $d = 3$ or 5 , and choose the number of variables as $p = 200$ or 500 . We use a small sample size of $n = 100$ for both training and tuning. The true number of principal components is treated as known. The empirical performances based on 100 repetitions of the experiments are summarized in Tables 1 and 2. Table 1 summarizes the potential of each method, while Table 2 shows the actual numerical performance with the automatic tuning parameter selection.

We note several observations from the simulation studies. First, POI solutions are potentially closer to the truth than Fast POI solutions. Second, as expected, our methods with coordinate-wise sparsity-inducing penalty (POI-C and FastPOI-C) work well for the coordinate-wise sparse models (I and III), especially for the larger subspace dimension

| Model | d | p | POI-L | POI-C | FastPOI-L | FastPOI-C | Zou et al. | Song et al. | Shen & Huang |
|-------|-----|-----|--------------|--------------|-----------|--------------|------------|--------------|--------------|
| I | 3 | 200 | 0.202 | 0.162 | 0.204 | 0.165 | 0.201 | 0.262 | 0.198 |
| | 3 | 500 | 0.204 | 0.152 | 0.213 | 0.159 | 0.211 | 0.292 | 0.205 |
| | 5 | 200 | 0.359 | 0.199 | 0.420 | 0.228 | 0.419 | 0.445 | 0.369 |
| | 5 | 500 | 0.482 | 0.209 | 0.651 | 0.378 | 0.443 | 0.576 | 0.397 |
| II | 3 | 200 | 0.111 | 0.163 | 0.159 | 0.162 | 0.130 | 0.107 | 0.109 |
| | 3 | 500 | 0.110 | 0.166 | 0.158 | 0.166 | 0.127 | 0.105 | 0.106 |
| | 5 | 200 | 0.284 | 0.538 | 0.354 | 0.459 | 0.293 | 0.276 | 0.232 |
| | 5 | 500 | 0.376 | 0.620 | 0.630 | 0.705 | 0.331 | 0.361 | 0.286 |
| III | 3 | 200 | 0.114 | 0.151 | 0.180 | 0.155 | 0.161 | 0.115 | 0.135 |
| | 3 | 500 | 0.125 | 0.156 | 0.197 | 0.162 | 0.169 | 0.124 | 0.146 |
| | 5 | 200 | 0.420 | 0.344 | 0.509 | 0.407 | 0.530 | 0.502 | 0.405 |
| | 5 | 500 | 0.537 | 0.355 | 0.741 | 0.558 | 0.554 | 0.588 | 0.435 |

Table 2: The projection distance from the cross-validated estimate, averaged from 100 repetitions, for principal subspace estimation. The standard errors are at most 0.027. Smaller distance indicates more precise estimation. Highlighted are the best performed models (within 2 standard error of the smallest).

$d = 5$. In contrast, the lasso-type penalty works well for Model II, the eigenvectors of which are strictly element-wise sparse. Finally, POI-C provides much more accurate estimates than the competing methods for coordinate-wise sparse models (Model I).

In terms of the variable selection performance of the estimates, POI-C and FastPOI-C are both clearly superior than any other methods for Model I, and are comparable to the best performing methods for Models II and III. Numerical results for the variable selection performance can be found in the online supplementary material.

4.2 Sparse Subspace Learning for Multiclass LDA

We now apply our algorithm in the estimation of sparse discriminating basis for multi-group data. Suppose that \mathbf{x} follows a K -mixture of multivariate normal distributions, each with mean $\boldsymbol{\mu}_i$ and a common variance $\boldsymbol{\Sigma}_i = \boldsymbol{\Sigma}$, for all $i = 1, \dots, K$, where $K > 1$. Assuming that the group membership y is also observed, write $\boldsymbol{\Sigma}_T = \text{Cov}(\mathbf{x})$ for the total-covariance matrix and $\boldsymbol{\Sigma}_W = \boldsymbol{\Sigma}$ for the within-group covariance matrix. The between-group covariance

matrix is $\Sigma_B = \Sigma_T - \Sigma_W$, whose rank is at most $K - 1$. Then the problem of finding the discriminant subspace is equivalent to the GEP with $\mathbf{A} = \Sigma_B$ and $\mathbf{B} = \Sigma_W$.

We demonstrate the performance of Fast POI, but not POI. There are three reasons for this. First of all, Fast POI is well-suited for the case where the rank of \mathbf{A} is known. In multiclass LDA, the rank of \mathbf{A} is typically $K - 1$. Second, the performance of Fast POI was comparable or even superior to that of POI in our preliminary numerical studies. Third, POI requires considerably longer computation times than Fast POI. The performance of Fast POI estimates are compared with recently proposed linear sparse classifiers (Clemmensen et al., 2011; Mai et al., 2017; Gaynanova et al., 2016).

To simulate data, we use mixtures of normal distributions $N(\boldsymbol{\mu}_i, \Sigma)$. We set the mean matrix $\boldsymbol{\mu} = (\boldsymbol{\mu}_1, \dots, \boldsymbol{\mu}_K)$ and Σ as follows. Throughout, the dimension is set to be $p = 200$. Let $C(\rho)$ be the compound symmetry covariance model: $C(\rho) = (1 - \rho)\mathbf{I}_p + \rho\mathbf{J}_p$, $\mathbf{J}_p = \mathbf{1}_p\mathbf{1}_p^\top$. Let $R(\rho)$ be the AR(1) model: $\{R(\rho)\}_{i,j} = \rho^{|i-j|}$. Define $\mathbf{V} = (\mathbf{v}_1, \mathbf{v}_2, \mathbf{v}_3)$ and $\mathbf{W} = (\mathbf{w}_1, \mathbf{w}_2, \mathbf{w}_3)$ by

$$\begin{aligned} \mathbf{v}_1^\top &= (2, 1, 2, 1, 2, 0, \dots, 0)_{1 \times p}, & \mathbf{w}_1^\top &= (-1, 1, 1, 1, 1, 0, \dots, 0)_{1 \times p}, \\ \mathbf{v}_2^\top &= (1, -1, 1, -1, 1, 0, \dots, 0)_{1 \times p}, & \mathbf{w}_2^\top &= (1, -1, 1, -1, 1, 0, \dots, 0)_{1 \times p}, \\ \mathbf{v}_3^\top &= (0, 1, -1, 1, 0, 0, \dots, 0)_{1 \times p}, & \mathbf{w}_3^\top &= (1, 1, -1, 1, 0, 0, \dots, 0)_{1 \times p}. \end{aligned}$$

Our models are given as follows. For Model I, $\boldsymbol{\mu} = (\boldsymbol{\mu}_1, \boldsymbol{\mu}_2, \boldsymbol{\mu}_3) = \mathbf{V}$, $\Sigma = \mathbf{I}_p$; Model II, $\boldsymbol{\mu} = \Sigma\mathbf{V}$, $\Sigma = C(0.5)$; Model III, $\boldsymbol{\mu} = \Sigma\mathbf{V}$, $\Sigma = R(0.5)$; Model IV, $\boldsymbol{\mu} = \Sigma\mathbf{W}$, $\Sigma = C(0.5)$; for Model V, let $\tilde{\mathbf{W}} = 2(\mathbf{w}_1, \mathbf{w}_2, \mathbf{w}_3, \bar{\mathbf{w}})$, where $\bar{\mathbf{w}} = (\mathbf{w}_1 + \mathbf{w}_2 + \mathbf{w}_3)/3$, and set $\boldsymbol{\mu} = (\boldsymbol{\mu}_1, \boldsymbol{\mu}_2, \boldsymbol{\mu}_3, \boldsymbol{\mu}_4) = \Sigma\tilde{\mathbf{W}}$, and $\Sigma = C(0.5)$.

The true generalized eigenvectors are given by solving the generalized eigenvector problem with $\mathbf{A} = \sum_{k=1}^K (\boldsymbol{\mu}_k - \bar{\boldsymbol{\mu}})(\boldsymbol{\mu}_k - \bar{\boldsymbol{\mu}})^\top / K$, where $\bar{\boldsymbol{\mu}} = \sum_{k=1}^K \boldsymbol{\mu}_k / K$, and $\mathbf{B} = \Sigma$. Note that although the eigenvectors are different for different models, the true subspaces in Models I–III are the same; they are all spanned by $\{\mathbf{v}_i - \mathbf{v}_j, : i \neq j\}$. Likewise, the true subspaces in Models IV and V are both spanned by $\{\mathbf{w}_i - \mathbf{w}_j, : i \neq j\}$. Since the basis of a subspace can only be coordinate-wise sparse, it is expected that coordinate-wise sparse estimates (including FastPOI-C and the method of Gaynanova et al. (2016)) work well. Our simulation result, reported below, concurs.

In Models I–IV, we need to estimate a subspace of dimension 2, since there are $K = 3$

groups. In Model V, we still need to estimate the 2-dimensional subspace, even though there are $K = 4$ groups. In principle, this information is not available to statisticians, and for all model estimation, we estimate the subspace of dimension $d = K - 1$; that is, the model is misspecified for Model V. Our simulation shows that our method works well for this case as well.

Our application to sparse LDA as well as the competing methods (Clemmensen et al., 2011; Mai et al., 2017; Gaynanova et al., 2016) first estimate sparse basis vectors, then apply multiclass LDA to the dimension-reduced data. Following their approaches, the standard LDA is applied to the data pair $(\mathbf{X}\hat{\mathbf{U}}, y)$ for the classification and prediction. From each model above, we generate a training set of size $n_i = 30$ (for each group), a tuning set of the same size, and a testing set of size $n = 100Kn_i$. Our tuning procedure, utilizing (14), is used for all methods. The testing set is used to estimate the misclassification rate. Experiments are repeated 100 times. We report the qualities of subspace learning and classification performance in Tables 3 and 4, respectively.

Table 3 shows that FastPOI-C provides most accurate estimates of the the true subspace. As explained above, it makes most sense to assume coordinate-wise sparsity in subspace learning. Thus the methods of Mai et al. (2017) and Clemmensen et al. (2011), seeking element-wise sparsity, are expected to be inferior in subspace learning. Likewise, the performance of FastPOI-L is inferior to that of FastPOI-C. Note that Gaynanova et al. (2016) also imposed the coordinate-wise sparsity, thus showing better performance in subspace learning than other method, except FastPOI-C.

The proposed FastPOI-C also performed the best in terms of classification. It is evident from Table 4 that FastPOI-C yields the smallest misclassification rates for Models I–IV, and is second to Gaynanova’s classifier for Model V. Given the similarity of FastPOI-C and Gaynanova’s (note Remark 2 and that they both seek coordinate-wise sparse solutions), it is expected that both perform well in classification.

An alternative tuning procedure, minimizing misclassification error rates in the special case of multiclass LDA, provides similar numerical performances. In fact, both choices of the tuning parameter are generally close to each other, as we have seen in Fig. 1. Fast POI tends to choose more variables than needed, but shows better sensitivity, i.e., more signal

| Model | FastPOI-L | FastPOI-C | Mai et al. | Clemmensen et al. | Gaynanova et al. |
|-------|--------------|--------------|------------|-------------------|------------------|
| I | 0.328 | 0.313 | 0.371 | 0.622 | 0.377 |
| II | 0.839 | 0.570 | 0.936 | 0.817 | 0.611 |
| III | 0.644 | 0.437 | 0.542 | 0.784 | 0.608 |
| IV | 0.852 | 0.478 | 0.916 | 0.689 | 0.514 |
| V | 0.712 | 0.359 | 0.869 | 0.365 | 0.411 |

Table 3: The projection distance from the estimate, averaged from 100 repetitions, for sparse discriminant basis learning. The standard errors are at most 0.024. Smaller distance indicates more precise estimation. Highlighted are the best performed models (within 2 standard error of the smallest).

| Model | FastPOI-L | FastPOI-C | Mai et al. | Clemmensen et al. | Gaynanova et al. |
|-------|-------------|--------------|------------|-------------------|------------------|
| I | 7.46 | 7.27 | 9.41 | 10.23 | 12.30 |
| II | 30.50 | 8.72 | 21.74 | 9.70 | 12.49 |
| III | 17.10 | 12.41 | 17.23 | 18.41 | 19.19 |
| IV | 35.84 | 16.03 | 23.62 | 18.00 | 19.68 |
| V | 32.40 | 16.13 | 26.80 | 16.57 | 15.98 |

Table 4: Misclassification rates (in percent) of the test set, averaged from 100 repetitions. The standard errors are at most 1.19. Smaller error rate indicates better classification. Highlighted are the best performed models (within 2 standard error of the smallest).

variables (or coordinates) are included in the estimates, than other methods. In terms of an overall variable selection performance, FastPOI-C and Gaynanova et al. (2016)’s method shows similar performances, while both are better than the others. Simulation results for the alternative choices of tuning parameters and for the variable selection performance can be found in the online supplementary material.

4.3 Sufficient Dimension Reduction

Sufficient dimension reduction (Cook, 2009) aims to find a projection of data \mathbf{x} that is sufficient for (i.e., preserves all information about) the conditional distribution of y given

\mathbf{x} . Many sufficient dimension reduction (SDR) methods can be cast into a GEP, as shown in Li (2007). In particular, the solution for the sliced inverse regression (SIR, Li, 1991), the most well-known method for SDR, is given by the eigenvectors of the GEP (1) where $\mathbf{A} = \text{Cov}[E\{\mathbf{x} - E(\mathbf{x})|y\}]$ and $\mathbf{B} = \text{Cov}(\mathbf{x})$. We apply our sparse solutions of GEP by POI-C to SIR for a benchmark data set. In all examples in this subsection, we used $\lambda = \lambda_{\max}/2$.

The Tai-Chi data have been sometimes used as a benchmark data for various methods of SDR, e.g., in Wu et al. (2009). For our purpose, we randomly generate (\mathbf{x}, y) pairs for $n = 1000$ times as shown in Fig. 3. The first two coordinates of $\mathbf{x} \in \mathbb{R}^p$ are uniformly sampled over the disk with radius 2, while the rest of coordinates are sampled from the standard normal distribution. The binary variable y depends on the location of \mathbf{x} , and is 1 if \mathbf{x} lies on the ‘yin’ part of the Tai-Chi symbol, 0 otherwise. The true subspace only spans over the first two coordinates.

For sufficient dimension reduction of the toy data, a direct competitor is Chen et al. (2010)’s sparse estimation for SIR. Note that Tan et al. (2016)’s method is not applicable to this data set as it only computes one eigenvector, while at least two eigenvectors are needed here. The method of Li (2007) is not compared, as Chen et al. (2010) improves upon Li (2007). Figure 3 displays the projected data onto the estimated subspaces from the original SIR and our adaptation of SIR with POI-C. The graphical result from Chen et al. (2010) is almost identical to POI-C, and both methods greatly improve upon the original SIR for this data set.

To further compare our approach with Chen et al. (2010)’s, we have repeated the experiment for various cases of sample size and dimension. It appears that Chen’s method requires large sample size to work well, and is numerically unstable for small sample sizes. Our method exhibits great performances for any case, and requires only a fraction of computation time compared to Chen’s. Relevant numerical results can be found in the online supplementary material.

4.4 Canonical Correlation Analysis

We briefly demonstrate an application of our methods to sparse canonical correlation analysis (CCA). It is well known that CCA can be viewed as a GEP (Gaynanova et al., 2017;

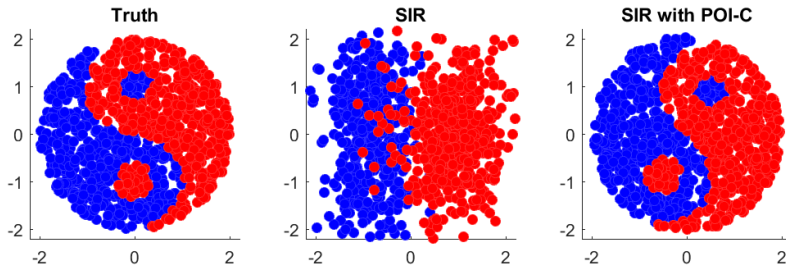


Figure 3: Projections of a Tai-Chi data set to the true subspace (left panel), the estimated subspace by the original SIR (Li, 1991, middle panel), SIR estimated by POI-C (right panel). The data set has $n = 1000$ observations, each with dimension $p = 500$.

Safo et al., 2018). The canonical coefficient vectors are defined as follows. For two random vectors $\mathbf{x} \in \mathbb{R}^p$, $\mathbf{y} \in \mathbb{R}^q$, write $\Sigma_1 = \text{Cov}(\mathbf{x})$, $\Sigma_2 = \text{Cov}(\mathbf{y})$ and $\Sigma_{12} = \text{Cov}(\mathbf{x}, \mathbf{y}) = \Sigma_{21}^T$. The coefficient vectors for the first pair of canonical variables are $(\mathbf{g}_1, \mathbf{h}_1) \in \mathbb{R}^p \times \mathbb{R}^q$, maximizing the correlation between $\mathbf{g}^T \mathbf{x}$ and $\mathbf{h}^T \mathbf{y}$: $\rho(\mathbf{g}, \mathbf{h}) = \mathbf{g}^T \Sigma_{12} \mathbf{h} / (\mathbf{g}^T \Sigma_1 \mathbf{g})^{\frac{1}{2}} (\mathbf{h}^T \Sigma_2 \mathbf{h})^{\frac{1}{2}}$. Since $\rho(\mathbf{g}, \mathbf{h})$ is invariant under individual scaling of (\mathbf{g}, \mathbf{h}) , a Lagrangian formulation of the maximization involves the condition $\mathbf{g}^T \Sigma_1 \mathbf{g} = \mathbf{h}^T \Sigma_2 \mathbf{h} = 1$, and the first-order condition of the Lagrangian coincides with the GEP (1) for

$$\mathbf{A} = \begin{pmatrix} \mathbf{0} & \Sigma_{12} \\ \Sigma_{21} & \mathbf{0} \end{pmatrix}, \quad \mathbf{B} = \begin{pmatrix} \Sigma_1 & \mathbf{0} \\ \mathbf{0} & \Sigma_2 \end{pmatrix}, \quad (23)$$

where the solution (\mathbf{u}, λ) corresponds to the concatenated coefficient vector $(\mathbf{g}^T, \mathbf{h}^T)^T$ and canonical correlation coefficient $\rho(\mathbf{g}, \mathbf{h})$, respectively. An alternative formulation of CCA is given by solving the GEP (23) with respect to individual \mathbf{g} or \mathbf{h} , leading to two GEPs:

$$\Sigma_{12} \Sigma_2^{-1} \Sigma_{21} \mathbf{g} = \lambda \Sigma_1 \mathbf{g}, \quad \Sigma_{21} \Sigma_1^{-1} \Sigma_{12} \mathbf{h} = \lambda \Sigma_2 \mathbf{h}. \quad (24)$$

In performing a sparse CCA, we use (24) as done in Safo et al. (2018). In the estimation of the pair (\mathbf{g}, \mathbf{h}) from a sample, we follow the suggestion from Witten et al. (2009) and Safo et al. (2018) of first standardizing the data, then replacing $\widehat{\Sigma}_1$ by \mathbf{I}_p and $\widehat{\Sigma}_2$ by \mathbf{I}_q . With the sample cross-covariance matrix $\widehat{\Sigma}_{12}$, we apply the POI in solving $\Sigma_{12} \Sigma_{12}^T \mathbf{g} = \lambda \mathbf{g}$ and $\Sigma_{12}^T \Sigma_{12} \mathbf{h} = \lambda \mathbf{h}$. Applying our method, or any existing general sparse GEP methods

(Sriperumbudur et al., 2011; Song et al., 2015), to the GEP (23) typically leads unsatisfactory results partly due to the fact that \mathbf{A} is not in general nonnegative definite and also because of different scales of $\mathbf{\Sigma}_1$ and $\mathbf{\Sigma}_2$. In a simulation study with $n = 80$ observations of two random vectors of dimension $p = 200, q = 150$, in which there is one canonical pair, the performance of POI estimates is comparable to the method of Safo et al. (2018), and are superior than the methods of Witten et al. (2009) and Gao et al. (2017). We refer to the online supplementary material for simulation settings and numerical results.

A Technical Details

Proof of Proposition 1. There exists a nonsingular matrix \mathbf{S} such that $\mathbf{U}_d = \tilde{\mathbf{Q}}_d \mathbf{S}$. The equation (4) is written as

$$\mathbf{A} \tilde{\mathbf{Q}}_d \mathbf{S} = \mathbf{B} \tilde{\mathbf{Q}}_d \mathbf{S} \mathbf{\Lambda}_d,$$

which yields

$$(\tilde{\mathbf{Q}}_d^T \mathbf{A} \tilde{\mathbf{Q}}_d) \mathbf{S} = (\tilde{\mathbf{Q}}_d^T \mathbf{B} \tilde{\mathbf{Q}}_d) \mathbf{S} \mathbf{\Lambda}_d,$$

moreover, we have $\mathbf{S}^T (\tilde{\mathbf{Q}}_d^T \mathbf{B} \tilde{\mathbf{Q}}_d) \mathbf{S} = \mathbf{U}_d^T \mathbf{B} \mathbf{U}_d = \mathbf{I}_d$. Therefore, \mathbf{S} and $\mathbf{\Lambda}_d$ respectively are the matrix of eigenvectors and the diagonal matrix of eigenvalues of the GEP problem (6). \square

The following elementary lemma is used in the proof of Proposition 2. We use the notation $\mathcal{C}(\mathbf{A})$ to denote the column space of matrix \mathbf{A} .

Lemma 4. *Let $\mathbf{M}, \mathbf{M}_1, \mathbf{M}_2 \in \mathbb{R}^{p \times d}, \mathbf{N} \in \mathbb{R}^{d \times d}, \mathbf{L} \in \mathbb{R}^{p \times p}$ and assume that both \mathbf{N}, \mathbf{L} are invertible.*

1. $\mathcal{C}(\mathbf{M}) = \mathcal{C}(\mathbf{M}\mathbf{N})$.
2. If $\mathcal{C}(\mathbf{M}_1) = \mathcal{C}(\mathbf{M}_2)$, then $\mathcal{C}(\mathbf{L}\mathbf{M}_1) = \mathcal{C}(\mathbf{L}\mathbf{M}_2)$.

We omit the proof of Lemma 4.

Proof of Proposition 2. Under Case (a), $\mathbf{B} = \mathbf{I}_p$, and the generalized eigen-equation becomes $\mathbf{A}\mathbf{Q}_d = \mathbf{Q}_d \mathbf{\Lambda}_d^*$. Thus $\mathbf{Q}_d = \mathbf{V}_d$ by definition, which in turn leads to $\mathcal{C}(\mathbf{B}^{-1}\mathbf{V}_d) = \mathcal{C}(\mathbf{V}_d) = \mathcal{C}(\mathbf{Q}_d)$.

For case (b), define $\mathbf{C} = \mathbf{B}^{-\frac{1}{2}}\mathbf{A}\mathbf{B}^{-\frac{1}{2}}$. Then the generalized eigen-equation rewrites to $\mathbf{C}\mathbf{B}^{\frac{1}{2}}\mathbf{Q}_d = \mathbf{B}^{\frac{1}{2}}\mathbf{Q}_d\mathbf{\Lambda}_d^*$. By the QR decomposition of $\mathbf{B}^{\frac{1}{2}}\mathbf{Q}_d$, there exist $\mathbf{Q}_d^\dagger \in \mathcal{O}(p, d)$ and a $k \times k$ upper-triangular matrix $\mathbf{\Lambda}_d^\dagger$ satisfying

$$\mathbf{C}\mathbf{Q}_d^\dagger = \mathbf{Q}_d^\dagger\mathbf{\Lambda}_d^\dagger. \quad (25)$$

Since $\text{rank}(\mathbf{C}) = k$, (25) is equivalent to

$$\mathbf{C}[\mathbf{Q}_d^\dagger, \mathbf{Q}_d^\perp] = [\mathbf{Q}_d^\dagger, \mathbf{Q}_d^\perp] \begin{pmatrix} \mathbf{\Lambda}_d^\dagger & \mathbf{0} \\ \mathbf{0} & \mathbf{0} \end{pmatrix}, \quad (26)$$

where $[\mathbf{Q}_d^\dagger, \mathbf{Q}_d^\perp] \in \mathcal{O}(p)$. Thus $\mathbf{C} = \mathbf{Q}_d^\dagger\mathbf{\Lambda}_d^\dagger(\mathbf{Q}_d^\dagger)^\top$, and we get $\mathcal{C}(\mathbf{C}) = \mathcal{C}(\mathbf{Q}_d^\dagger) = \mathcal{C}(\mathbf{B}^{\frac{1}{2}}\mathbf{Q}_d)$. (These are obtained by the definition of eigendecomposition and QR decomposition.) On the other hand, using Lemma 4, it can be shown that $\mathcal{C}(\mathbf{B}^{\frac{1}{2}}\mathbf{B}^{-1}\mathbf{V}_d) = \mathcal{C}(\mathbf{B}^{-\frac{1}{2}}\mathbf{V}_d) = \mathcal{C}(\mathbf{B}^{-\frac{1}{2}}\mathbf{A}\mathbf{B}^{-\frac{1}{2}}) = \mathcal{C}(\mathbf{C})$.

Since $\mathbf{B}^{\frac{1}{2}}$ is invertible and $\mathcal{C}(\mathbf{B}^{\frac{1}{2}}\mathbf{B}^{-1}\mathbf{V}_d) = \mathcal{C}(\mathbf{B}^{\frac{1}{2}}\mathbf{Q}_d)$, again by Lemma 4, we conclude that $\mathcal{C}(\mathbf{B}^{-1}\mathbf{V}_d) = \mathcal{C}(\mathbf{Q}_d)$. \square

Proof of Lemma 3. Notice that each optimization problem is column-wise separable. Each column-wise subproblem is then a least-square problem. \square

Acknowledgements

Jeon's research was supported by Basic Science Research Program of the National Research Foundation of Korea (NRF-2015R1A1A1A05001180) funded by the Korean government.

SUPPLEMENTARY MATERIAL

Additional analysis: Document containing an extensive list of statistical GEP problems and additional numerical results. (.pdf file)

Matlab routine: Matlab functions that perform the sparse generalized eigenvector estimation as described in the article. (Compressed files .zip) The files are also available at <https://github.com/sungkyujung/SparseEIG>

References

- Bouveyron, C., P. Latouche, and P.-A. Mattei (2016). Bayesian variable selection for globally sparse probabilistic PCA. Preprint HAL 01310409, Université Paris Descartes. arXiv:1605.05918.
- Caliński, T. and J. Harabasz (1974). A dendrite method for cluster analysis. *Communications in Statistics-theory and Methods* 3(1), 1–27.
- Chen, X., C. Zou, R. D. Cook, et al. (2010). Coordinate-independent sparse sufficient dimension reduction and variable selection. *The Annals of Statistics* 38(6), 3696–3723.
- Ciriello, G., M. L. Gatzka, A. H. Beck, M. D. Wilkerson, S. K. Rhie, A. Pastore, H. Zhang, M. McLellan, C. Yau, C. Kandoth, et al. (2015). Comprehensive molecular portraits of invasive lobular breast cancer. *Cell* 163(2), 506–519.
- Clemmensen, L., T. Hastie, D. Witten, and B. Ersbll (2011). Sparse discriminant analysis. *Technometrics* 53(4), 406–413.
- Cook, R. D. (2009). *Regression graphics: Ideas for studying regressions through graphics*, Volume 482. John Wiley & Sons.
- Gao, C., Z. Ma, H. H. Zhou, et al. (2017). Sparse cca: Adaptive estimation and computational barriers. *The Annals of Statistics* 45(5), 2074–2101.
- Gaynanova, I., J. G. Booth, and M. T. Wells (2016). Simultaneous sparse estimation of canonical vectors in the $p \gg n$ setting. *Journal of the American Statistical Association* 111(514), 696–706.
- Gaynanova, I., J. G. Booth, and M. T. Wells (2017). Penalized versus constrained generalized eigenvalue problems. *Journal of Computational and Graphical Statistics* 26(2), 379–387.
- Golub, G. H. and C. F. Van Loan (1996). *Matrix computations* (Third ed.). Baltimore: JHU Press.

- Han, X. and L. Clemmensen (2016). Regularized generalized eigen-decomposition with applications to sparse supervised feature extraction and sparse discriminant analysis. *Pattern Recognition* 49, 43–54.
- Hastie, T., R. Tibshirani, and J. Friedman (2009). *Elements of Statistical Learning*. New York: Springer-Verlag.
- Johnstone, I. M. and A. Y. Lu (2009). On Consistency and Sparsity for Principal Components Analysis in High Dimensions. *Journal of the American Statistical Association* 104(486), 682–693.
- Josse, J. and F. Husson (2012). Selecting the number of components in principal component analysis using cross-validation approximations. *Computational Statistics & Data Analysis* 56(6), 1869–1879.
- Jung, S. and J. S. Marron (2009, December). PCA consistency in high dimension, low sample size context. *Ann. Stat.* 37(6B), 4104–4130.
- Kokiopoulou, E., J. Chen, and Y. Saad (2011). Trace optimization and eigenproblems in dimension reduction methods. *Numerical Linear Algebra with Applications* 18(3), 565–602.
- Li, K.-C. (1991). Sliced inverse regression for dimension reduction (with discussion). *Journal of the American Statistical Association* 86(414), 316–342.
- Li, L. (2007). Sparse sufficient dimension reduction. *Biometrika* 94(3), 603–613.
- Ma, Z. (2013). Sparse principal component analysis and iterative thresholding. *The Annals of Statistics* 41(2), 772–801.
- Mai, Q., Y. Yang, and H. Zou (2017). Multiclass sparse discriminant analysis. *Statistica Sinica* (to appear). arXiv:1504.05845.
- Safo, S. E., J. Ahn, Y. Jeon, and S. Jung (2018). Sparse generalized eigenvalue problem with application to canonical correlation analysis for integrative analysis of methylation and gene expression data. *Biometrics in press*.

- Shen, H. and J. Z. Huang (2008). Sparse principal component analysis via regularized low rank matrix approximation. *Journal of multivariate analysis* 99(6), 1015–1034.
- Song, J., P. Babu, and D. P. Palomar (2015). Sparse generalized eigenvalue problem via smooth optimization. *IEEE Transactions on Signal Processing* 63(7), 1627–1642.
- Sriperumbudur, B. K., D. A. Torres, and G. R. Lanckriet (2011). A majorization-minimization approach to the sparse generalized eigenvalue problem. *Machine learning* 85(1-2), 3–39.
- Tan, K. M., Z. Wang, H. Liu, and T. Zhang (2016). Sparse generalized eigenvalue problem: optimal statistical rates via truncated Rayleigh flow. *arXiv preprint arXiv:1604.08697*.
- Tibshirani, R. (1996). Regression shrinkage and selection via the lasso. *Journal of the Royal Statistical Society: Series B (Statistical Methodology)* 58(1), 267–288.
- Tibshirani, R. (2011). Regression shrinkage and selection via the lasso: a retrospective. *Journal of the Royal Statistical Society: Series B (Statistical Methodology)* 73(3), 273–282.
- Tseng, P. (1993). Dual coordinate ascent methods for non-strictly convex minimization. *Mathematical Programming* 59(1-3), 231–247.
- Tyler, D. E., F. Critchley, L. Dümbgen, and H. Oja (2009). Invariant co-ordinate selection. *Journal of the Royal Statistical Society: Series B (Statistical Methodology)* 71(3), 549–592.
- Witten, D. M., R. Tibshirani, and T. Hastie (2009). A penalized matrix decomposition, with applications to sparse principal components and canonical correlation analysis. *Biostatistics* 10(3), 515–534.
- Wu, M., L. Zhang, Z. Wang, D. Christiani, and X. Lin (2009). Sparse linear discriminant analysis for simultaneous testing for the significance of a gene set/pathway and gene selection. *Bioinformatics* 25(9), 1145–1151.

- Yuan, M. and Y. Lin (2006). Model selection and estimation in regression with grouped variables. *Journal of the Royal Statistical Society: Series B (Statistical Methodology)* 68(1), 49–67.
- Zhang, Z., T. W. Chow, and M. Zhao (2013). Trace ratio optimization-based semi-supervised nonlinear dimensionality reduction for marginal manifold visualization. *IEEE Transactions on Knowledge and Data Engineering* 25(5), 1148–1161.
- Zou, H., T. Hastie, and R. Tibshirani (2006). Sparse principal component analysis. *Journal of Computational and Graphical Statistics* 15(2), 265–286.

Supplementary material: Penalized Orthogonal Iteration for Sparse Estimation of Generalized Eigenvalue Problem

Sungkyu Jung
Department of Statistics, University of Pittsburgh
Jeongyoun Ahn
Department of Statistics, University of Georgia
and
Yongho Jeon
Department of Applied Statistics, Yonsei University

June 26, 2018

Contents

| | |
|--|-----------|
| S1 Supplement to Section 1: Generalized eigenvalue problems in statistics | 2 |
| S1.1 Linear dimension reduction | 2 |
| S1.2 Group mean difference and classification | 3 |
| S1.3 Canonical correlation analysis | 4 |
| S1.4 Nonlinear dimension reduction | 5 |
| S2 Supplement to Section 4.1: Variable selection performance in PCA | 6 |
| S3 Supplement to Section 4.2: Multiclass LDA | 11 |
| S3.1 Variable selection performance | 11 |
| S3.2 Extension of main article Tables 2 and 4 | 11 |
| S4 Supplement to Section 4.3: Sufficient dimension reduction | 14 |
| S5 Supplement to Section 4.4: Canonical correlation analysis | 15 |
| S6 Supplement to Section 4: Genomic data analysis | 16 |
| S6.1 Feature selection by sparse principal component analysis | 17 |

S1 Supplement to Section 1: Generalized eigenvalue problems in statistics

A number of multivariate statistical methods can be formulated into a generalized eigenvalue problem (GEP). As referenced in the main article Section 1, we list a few examples of the data-analytic situations and methods that can be cast into a GEP, and for each situation discuss existing approaches for sparse solutions.

S1.1 Linear dimension reduction

Linear dimension reduction finds linear combinations of variables that span a lower-dimensional subspace for data \mathbf{X} . The *principal component analysis (PCA)* is a prime example.

Example 1 (PCA). Let a random vector \mathbf{x} has the covariance matrix $\mathbf{\Sigma}$. It is well-known that the principal components are given by the eigen-decomposition of $\mathbf{\Sigma}$. By setting $\mathbf{A} = \mathbf{\Sigma}$, $\mathbf{B} = \mathbf{I}_p$, the problem

$$\mathbf{A}\mathbf{u}_j = \lambda_j\mathbf{B}\mathbf{u}_j, \tag{S1}$$

becomes the ordinary eigen-decomposition problem, and the solution $(\mathbf{u}_j, \lambda_j)$ corresponds to the principal component (PC) direction and variance pair.

There have been a number of proposals for sparse PCA; to name a few, Jolliffe et al. (2003); Zou et al. (2006); d’Aspremont et al. (2008); Shen and Huang (2008); Witten et al. (2009); Ma (2013); Bouveyron et al. (2016). Theoretical guarantees for some of the sparse PCA methods have been given in e.g., Shen et al. (2013) and Ma (2013). In computing sparse PCs, most of these methods utilized the fact that the original data matrix \mathbf{X} is available, and proposed to modify the standard singular value decomposition (e.g., Shen and Huang, 2008; Witten et al., 2009) or forming a penalized regression problem (e.g., Zou et al., 2006). In contrast, we focus on solving the GEP directly, thus require computing the sample covariance matrix $\widehat{\mathbf{\Sigma}}$ as an input to our algorithm. As pointed out in Remark 1 (in the main article), a special case of our proposal coincides with the method of Ma (2013), in which $\widehat{\mathbf{\Sigma}}$ is also used, and the method is shown to be consistent in a high-dimensional sparse setting.

Some extensions of PCA and factor models that incorporate structures in the data (Jenatton et al., 2010; Allen et al., 2014; Lock et al., 2013; Li and Jung, 2017) have a potential to be cast into a GEP, by e.g. formulating the \mathbf{B} matrix according to the structure given a priori.

Invariant co-ordinate selection (ICS, Tyler et al., 2009) is a general framework, examples of which includes the linear discriminant analysis and the independent component analysis (Hyvärinen et al., 2004). Since the coordinates of ICS are precisely given by the generalized eigenvectors of a pair of general scatter matrices, our algorithm may be used as a sparse estimation method for ICS.

Many moment-based *sufficient dimension reduction* (SDR) methods can also be formulated as a GEP, as shown by Li (2007). As an example, we provide a GEP formulation of the sliced inverse regression (SIR, Li, 1991), the most well-known method of SDR.

Example 2 (SDR). Consider the regression of a univariate response y on p -variate predictor \mathbf{x} . SDR aims to find a projection of data \mathbf{x} that is sufficient for (i.e., preserves all information about) the conditional distribution of y given \mathbf{x} . By setting $\mathbf{A} = \text{Cov}[E\{\mathbf{x} - E(\mathbf{x})|y\}]$ and $\mathbf{B} = \text{Cov}(\mathbf{x})$, the eigenvectors of the GEP, equation (S1), span exactly the predictor subspace given by SIR.

We refer to Cook (2009), Li (2007) and Chen et al. (2010) for various SDR approaches and their relation to the generalized eigenvalue problem.

S1.2 Group mean difference and classification

Suppose that \mathbf{x} follows a K -mixture of multivariate normal distributions, each with mean $\boldsymbol{\mu}_i$ and a common variance $\boldsymbol{\Sigma}_i = \boldsymbol{\Sigma}$, for all $i = 1, \dots, K$, where $K > 1$. Assuming that the group membership y is also observed, common multivariate analyses incurred are classification of observations and testing the hypothesis of equal means.

Example 3 (Multiclass linear discriminant analysis (LDA)). Write $\boldsymbol{\Sigma}_T = \text{Cov}(\mathbf{x})$ for the total-covariance matrix and $\boldsymbol{\Sigma}_W = \boldsymbol{\Sigma}$ for the within-covariance matrix. The between-covariance matrix is $\boldsymbol{\Sigma}_B = \boldsymbol{\Sigma}_T - \boldsymbol{\Sigma}_W$, whose rank is at most $K - 1$. The multiclass LDA finds a discriminant subspace whose basis vectors \mathbf{u}_j are sequentially obtained by maximizing the Rayleigh coefficient:

$$T(\mathbf{u}) = \mathbf{u}^T \boldsymbol{\Sigma}_B \mathbf{u} / \mathbf{u}^T \boldsymbol{\Sigma}_W \mathbf{u}. \tag{S2}$$

This problem is equivalent to the GEP with $\mathbf{A} = \boldsymbol{\Sigma}_B$ and $\mathbf{B} = \boldsymbol{\Sigma}_W$.

There are vast literature on sparse estimation of the linear discriminant rule in high dimensions (Cai and Liu, 2011; Shao et al., 2011; Clemmensen et al., 2011; Mai et al., 2012, 2017; Witten and Tibshirani, 2011; Gaynanova et al., 2016). Witten and Tibshirani (2011) have noticed that the LDA direction in the binary classification is the solution of (S2), and proposed to solve a penalized GEP of the form

$$\max_{\mathbf{u}} \mathbf{u}^T \mathbf{A} \mathbf{u} - p_\rho(\mathbf{u}), \quad \text{subject to } \mathbf{u}^T \mathbf{B} \mathbf{u} = 1,$$

with the lasso or fused lasso penalty for p_ρ . Clemmensen et al. (2011), Mai et al. (2017) and Gaynanova et al. (2016) focused on the multi-category classification and aimed to estimate the discriminating subspace, similar to us. While Clemmensen et al. (2011) turned the classification problem into a regression setting, thus used the original data matrix \mathbf{X} , the methods of Mai et al. (2017) and Gaynanova et al. (2016) are based on the empirical versions of $\boldsymbol{\Sigma}_B$ and $\boldsymbol{\Sigma}_W$. Their objective functions are thus similar to that of our Fast POI; detailed discussion on the similarity can be found in Remark 2 in Section 2.2.2 (in the main article).

In the multiple population situation, the *Multivariate analysis of variance (MANOVA)* provides a simple means of testing the hypothesis $H_0 : \boldsymbol{\mu}_1 = \cdots = \boldsymbol{\mu}_K$, based on the between-covariance matrix $\boldsymbol{\Sigma}_B$ and the within-covariance matrix $\boldsymbol{\Sigma}_W$. Among the choices of test statistics for MANOVA are functions of the generalized eigenvalues λ_j , from the GEP with (S2), replacing $\boldsymbol{\Sigma}_B$ and $\boldsymbol{\Sigma}_W$ by the empirical counterparts. For example, Roy's test statistic is $\lambda_1 = \max(\lambda_j)$, and the Lawley-Hotelling statistic is $\sum_{j=1}^{K-1} \lambda_j$. The test of MANOVA rejects H_0 for larger values of test statistics. Sparse MANOVA using our proposal is not considered in the present paper, but is an interesting future work.

S1.3 Canonical correlation analysis

Canonical correlation analysis (CCA) can be thought of as a special case of linear dimension reduction.

Example 4 (Canonical correlation analysis (CCA)). Let \mathbf{x}, \mathbf{y} be two random vectors of dimensions p and q , respectively. Write $\boldsymbol{\Sigma}_1 = \text{Cov}(\mathbf{x})$, $\boldsymbol{\Sigma}_2 = \text{Cov}(\mathbf{y})$ and $\boldsymbol{\Sigma}_{12} = \text{Cov}(\mathbf{x}, \mathbf{y}) = \boldsymbol{\Sigma}_{21}^T$. The coefficient vectors for the first pair of canonical variables are $(\mathbf{g}_1, \mathbf{h}_1) \in \mathbb{R}^p \times \mathbb{R}^q$, maximizing the correlation between $\mathbf{g}_1^T \mathbf{x}$ and $\mathbf{h}_1^T \mathbf{y}$:

$$\text{Corr}(\mathbf{g}_1^T \mathbf{x}, \mathbf{h}_1^T \mathbf{y}) := \rho(\mathbf{g}, \mathbf{h}) = \frac{\mathbf{g}^T \boldsymbol{\Sigma}_{12} \mathbf{h}}{(\mathbf{g}^T \boldsymbol{\Sigma}_1 \mathbf{g})^{\frac{1}{2}} (\mathbf{h}^T \boldsymbol{\Sigma}_2 \mathbf{h})^{\frac{1}{2}}}. \quad (\text{S3})$$

Note that $\rho(\mathbf{g}, \mathbf{h})$ is invariant under individual scaling of (\mathbf{g}, \mathbf{h}) . Using this invariance, a Lagrangian formulation of the maximization involves the condition $\mathbf{g}^T \boldsymbol{\Sigma}_1 \mathbf{g} = \mathbf{h}^T \boldsymbol{\Sigma}_2 \mathbf{h} = 1$. The first-order condition for the stationary points of the Lagrangian coincides with the GEP,

$$\begin{pmatrix} \mathbf{0} & \boldsymbol{\Sigma}_{12} \\ \boldsymbol{\Sigma}_{21} & \mathbf{0} \end{pmatrix} \mathbf{u} = \lambda \begin{pmatrix} \boldsymbol{\Sigma}_1 & \mathbf{0} \\ \mathbf{0} & \boldsymbol{\Sigma}_2 \end{pmatrix} \mathbf{u}, \quad (\text{S4})$$

where the solution (\mathbf{u}, λ) corresponds to the concatenated coefficient vector $(\mathbf{g}_j^T, \mathbf{h}_j^T)^T$ and canonical correlation coefficient $\rho(\mathbf{g}_j, \mathbf{h}_j)$, respectively. An alternative formulation of CCA is given by solving the GEP (S4) with respect to either \mathbf{g}_j or \mathbf{h}_j , thus leading to two GEPs:

$$\boldsymbol{\Sigma}_{12} \boldsymbol{\Sigma}_2^{-1} \boldsymbol{\Sigma}_{21} \mathbf{g} = \lambda \boldsymbol{\Sigma}_1 \mathbf{g}, \quad \boldsymbol{\Sigma}_{21} \boldsymbol{\Sigma}_1^{-1} \boldsymbol{\Sigma}_{12} \mathbf{h} = \lambda \boldsymbol{\Sigma}_2 \mathbf{h}. \quad (\text{S5})$$

Sparse CCA has recently gained attention. See Witten et al. (2009); Safo et al. (2018); Chen et al. (2018); Gao et al. (2017) and references therein. Among those, it appears that Safo et al. (2018) is the only attempt to use sparse solutions of GEP as estimates for CCA. Witten et al. (2009)’s approach, solving (S3) directly with constraints on \mathbf{g} and \mathbf{h} , can be understood as a regularized generalized singular value decomposition (Van Loan, 1976), thus is not equivalent to a GEP. Chen et al. (2018) proposed to modify the power method, a standard numerical algorithm for eigen-decomposition, by transforming the GEP into the standard eigenvalue problem.

S1.4 Nonlinear dimension reduction

Nonlinear dimension reduction methods, such as locally linear embedding, Laplacian eigenmaps, multi-dimensional scaling, and ISOMAP, come down to solving a GEP. Detailed expositions can be found in Kokiopoulou et al. (2011) and references therein.

We point out that our methods may not be immediately applicable to these problem. For example, a number of manifold learning methods are formulated as an n -dimensional GEP, where the matrices \mathbf{A} and \mathbf{B} contain the pairwise distances between observations. In such a case, the assumption of sparse loading translates to zero pairwise distances between many observations, which does not seem to be natural. Therefore it is not advisable to apply any sparse learning directly, not at least with a careful modification.

S2 Supplement to Section 4.1: Variable selection performance in PCA

The following measures are used in gauging the variable selection performance of generalized eigenvector estimates.

Let $\mathbf{U} = (u_{ij})$ be the $p \times d$ matrix of true eigenvectors, and $\hat{\mathbf{U}} = (\hat{u}_{ij})$ be its estimate of the same size. Note that if the i th variable (or the i th coordinate) is a signal variable if $u_{ij} \neq 0$ for one or more $j = 1, \dots, d$, and is a non-signal variable if $u_{ij} = 0$ for all j . Thus, to measure the variable selection performance, for any matrix \mathbf{V} , the set of “positive” indices is defined by for $\epsilon \geq 0$,

$$s_\epsilon(\mathbf{V}) = \{i : \sum_{j=1}^d v_{ij}^2 > \epsilon, i = 1, \dots, p\},$$

and the set of “negative” indices by

$$s_\epsilon^C(\mathbf{V}) = \{i : \sum_{j=1}^d v_{ij}^2 \leq \epsilon, i = 1, \dots, p\}.$$

Note that $s_\epsilon(\mathbf{V}) \cup s_\epsilon^C(\mathbf{V}) = \{1, \dots, p\}$ for any $p \times d$ matrix \mathbf{V} . For the truth \mathbf{U} and an estimate $\hat{\mathbf{U}}$, we compute $s_0(\mathbf{U})$ and $s_\epsilon(\hat{\mathbf{U}})$ for $\epsilon = 10^{-10}$, which then leads to the following:

1. Total positive: $P = \#s_\epsilon(\hat{\mathbf{U}})$,
2. True positive: $TP = \#s_0(\mathbf{U}) \cap s_\epsilon(\hat{\mathbf{U}})$,

From the false positive count, $FP = \#s_0^C(\mathbf{U}) \cap s_\epsilon(\hat{\mathbf{U}})$, the true negative count, $TN = \#s_0^C(\mathbf{U}) \cap s_\epsilon^C(\hat{\mathbf{U}})$, the false negative count, $FN = \#s_0(\mathbf{U}) \cap s_\epsilon^C(\hat{\mathbf{U}})$ and the total negative count, $N = \#s_\epsilon^C(\hat{\mathbf{U}}) = TN + FN$, we compute

3. Sensitivity: TP/P ,
4. Specificity: TN/N ,
5. Matthews correlation coefficient: $\frac{TP \times TN - FP \times FN}{[P(TP + FN)(TN + FP)N]^{1/2}}$

It may be of interest to inspect the sparsity patterns of $\hat{\mathbf{U}}$ in terms of each element of $\hat{\mathbf{U}}$. For this, instead of inspecting the row ℓ_2 norms of the matrix, we define the set of positive “loadings” of the matrix \mathbf{V} by $s_\epsilon(\text{vec}(\mathbf{V}))$, where $\text{vec}(\mathbf{V})$ “vectorizes” \mathbf{V} by stacking the

column vectors vertically (i.e. $\text{vec}(\mathbf{V})$ is a matrix of size $(pd) \times 1$). The five measures defined above can be now used to extract the loading-wise sparsity pattern.

From the simulation studies in Section 4.1 (of the main article), we have computed the five measures of variable selection performance, both in terms of coordinate-wise sparsity and the loading-wise sparsity, for each method considered. The performances of the cross-validated estimates are presented in Tables S1, S2 and S3 based on 100 repetition.

As noted in the main article, FastPOI-C shows the best variable selection performance for Model I, while POI-C is a close contender; see Table S1. We note that both POI-L and FastPOI-L tend to include more variables, and also more loadings, than needed, indicated by low specificity. The solutions of POI-L and FastPOI-L are in general not element-wise sparse. This may be counter-intuitive, but is not. Since we utilize the QR decomposition in the POI algorithm, column-specific sparse loadings are not preserved.

The eigenvectors for Models II and III are specifically designed to reduce the effect of QR decomposition in the algorithm in destroying column-specific sparsity patterns; the QR decomposition of the true (element-wise sparse) eigenvector matrix results in the same, element-wise sparse, matrix. In Tables S2 and S3, we find that POI-C and POI-L (or FastPOI-L and FastPOI-C) have similar variable selection performances. For Model II, Shen and Huang (2008)'s method performed the best while our methods are comparable to it; for Model III, POI-L, FastPOI-C and Shen and Huang (2008)'s method performed comparable to each other.

Note that Song et al. (2015)'s method did not provide a sparse estimate, when tuned by our tuning procedure. We checked that by choosing a large tuning parameter λ , Song et al. (2015)'s estimate is sparse, but the quality of estimate become progressively worse for larger values of λ .

| Model I ($d = 3, p = 200$) | | POI-L | POI-C | FastPOI-L | FastPOI-C | Zou et al. | Song et al. | Shen & Huang |
|------------------------------|-------------|--------|--------|-----------|-----------|------------|-------------|--------------|
| Coord. | Total pos. | 56.50 | 30.12 | 44.18 | 28.95 | 50.65 | 200.00 | 50.53 |
| | True pos. | 10.00 | 10.00 | 10.00 | 10.00 | 10.00 | 10.00 | 10.00 |
| | Sensitivity | 1.00 | 1.00 | 1.00 | 1.00 | 1.00 | 1.00 | 1.00 |
| | Specificity | 0.76 | 0.89 | 0.82 | 0.90 | 0.79 | 0.00 | 0.79 |
| | Matthews | 0.39 | 0.59 | 0.46 | 0.59 | 0.42 | 0.00 | 0.42 |
| Loading | Total pos. | 169.50 | 90.36 | 132.54 | 86.85 | 68.48 | 403.16 | 68.01 |
| | True pos. | 30.00 | 30.00 | 30.00 | 30.00 | 23.99 | 23.16 | 23.63 |
| | Sensitivity | 1.00 | 1.00 | 1.00 | 1.00 | 0.80 | 0.77 | 0.79 |
| | Specificity | 0.76 | 0.89 | 0.82 | 0.90 | 0.92 | 0.33 | 0.92 |
| | Matthews | 0.39 | 0.59 | 0.46 | 0.59 | 0.52 | 0.05 | 0.51 |
| Model I ($d = 5, p = 500$) | | POI-L | POI-C | FastPOI-L | FastPOI-C | Zou et al. | Song et al. | Shen & Huang |
| Coord. | Total pos. | 109.01 | 21.86 | 63.45 | 18.37 | 61.51 | 500.00 | 48.69 |
| | True pos. | 10.00 | 10.00 | 10.00 | 10.00 | 10.00 | 10.00 | 10.00 |
| | Sensitivity | 1.00 | 1.00 | 1.00 | 1.00 | 1.00 | 1.00 | 1.00 |
| | Specificity | 0.80 | 0.98 | 0.89 | 0.98 | 0.89 | 0.00 | 0.92 |
| | Matthews | 0.30 | 0.74 | 0.44 | 0.78 | 0.48 | 0.00 | 0.53 |
| Loading | Total pos. | 545.05 | 109.30 | 317.25 | 91.85 | 91.07 | 2002.96 | 75.53 |
| | True pos. | 50.00 | 50.00 | 50.00 | 50.00 | 34.76 | 42.96 | 34.32 |
| | Sensitivity | 1.00 | 1.00 | 1.00 | 1.00 | 0.70 | 0.86 | 0.69 |
| | Specificity | 0.80 | 0.98 | 0.89 | 0.98 | 0.98 | 0.20 | 0.98 |
| | Matthews | 0.30 | 0.74 | 0.44 | 0.78 | 0.56 | 0.02 | 0.59 |

Table S1: Measures of variable selection performance of the cross-validated estimates, based on the simulations for PCA model I. See text for description of the measures and methods involved. Shown are averages from 100 repetitions. For Tables S1, S2 and S3, the standard errors of the total positive and true positive counts are at most 17.5 and 3.5, respectively; the standard errors of the sensitivity, specificity, and Matthews correlation coefficient are at most 0.03.

| Model II ($d = 3, p = 200$) | | POI-L | POI-C | FastPOI-L | FastPOI-C | Zou et al. | Song et al. | Shen & Huang |
|-------------------------------|-------------|--------|--------|-----------|-----------|------------|-------------|--------------|
| Coord. | Total pos. | 20.94 | 23.01 | 21.58 | 21.71 | 24.04 | 200.00 | 19.45 |
| | True pos. | 15.00 | 15.00 | 15.00 | 15.00 | 15.00 | 15.00 | 15.00 |
| | Sensitivity | 1.00 | 1.00 | 1.00 | 1.00 | 1.00 | 1.00 | 1.00 |
| | Specificity | 0.97 | 0.96 | 0.96 | 0.96 | 0.95 | 0.00 | 0.98 |
| | Matthews | 0.87 | 0.82 | 0.86 | 0.84 | 0.84 | 0.00 | 0.90 |
| Loading | Total pos. | 62.82 | 69.03 | 64.74 | 65.13 | 31.40 | 405.00 | 21.04 |
| | True pos. | 15.00 | 15.00 | 15.00 | 15.00 | 13.30 | 14.10 | 12.53 |
| | Sensitivity | 1.00 | 1.00 | 1.00 | 1.00 | 0.89 | 0.94 | 0.84 |
| | Specificity | 0.92 | 0.91 | 0.91 | 0.91 | 0.97 | 0.33 | 0.99 |
| | Matthews | 0.49 | 0.46 | 0.48 | 0.47 | 0.66 | 0.09 | 0.72 |
| Model II ($d = 5, p = 500$) | | POI-L | POI-C | FastPOI-L | FastPOI-C | Zou et al. | Song et al. | Shen & Huang |
| Coord. | Total pos. | 76.37 | 88.74 | 42.60 | 40.25 | 56.71 | 500.00 | 43.68 |
| | True pos. | 24.46 | 24.17 | 24.02 | 24.04 | 24.65 | 25.00 | 24.71 |
| | Sensitivity | 0.98 | 0.97 | 0.96 | 0.96 | 0.99 | 1.00 | 0.99 |
| | Specificity | 0.89 | 0.86 | 0.96 | 0.97 | 0.93 | 0.00 | 0.96 |
| | Matthews | 0.59 | 0.55 | 0.77 | 0.78 | 0.71 | 0.00 | 0.81 |
| Loading | Total pos. | 381.85 | 443.70 | 213.00 | 201.25 | 71.85 | 2004.95 | 48.79 |
| | True pos. | 24.46 | 24.17 | 24.02 | 24.04 | 22.14 | 24.29 | 21.81 |
| | Sensitivity | 0.98 | 0.97 | 0.96 | 0.96 | 0.89 | 0.97 | 0.87 |
| | Specificity | 0.86 | 0.83 | 0.92 | 0.93 | 0.98 | 0.20 | 0.99 |
| | Matthews | 0.26 | 0.24 | 0.34 | 0.34 | 0.58 | 0.04 | 0.69 |

Table S2: Measures of variable selection performance of the cross-validated estimates, based on the simulations for PCA model II. See text for description of the measures and methods involved. Shown are averages from 100 repetitions.

| Model III ($d = 3, p = 200$) | | POI-L | POI-C | FastPOI-L | FastPOI-C | Zou et al. | Song et al. | Shen & Huang |
|--------------------------------|-------------|--------|--------|-----------|-----------|------------|-------------|--------------|
| Coord. | Total pos. | 17.16 | 21.42 | 26.41 | 20.69 | 24.86 | 200.00 | 23.08 |
| | True pos. | 15.00 | 15.00 | 15.00 | 15.00 | 15.00 | 15.00 | 15.00 |
| | Sensitivity | 1.00 | 1.00 | 1.00 | 1.00 | 1.00 | 1.00 | 1.00 |
| | Specificity | 0.99 | 0.97 | 0.94 | 0.97 | 0.95 | 0.00 | 0.96 |
| | Matthews | 0.95 | 0.85 | 0.77 | 0.87 | 0.83 | 0.00 | 0.87 |
| Loading | Total pos. | 56.38 | 69.04 | 83.88 | 66.87 | 43.97 | 405.57 | 34.56 |
| | True pos. | 45.00 | 45.00 | 45.00 | 45.00 | 32.25 | 33.92 | 24.86 |
| | Sensitivity | 1.00 | 1.00 | 1.00 | 1.00 | 0.72 | 0.75 | 0.55 |
| | Specificity | 0.98 | 0.96 | 0.93 | 0.96 | 0.98 | 0.33 | 0.98 |
| | Matthews | 0.89 | 0.80 | 0.73 | 0.81 | 0.72 | 0.04 | 0.63 |
| Model III ($d = 5, p = 500$) | | POI-L | POI-C | FastPOI-L | FastPOI-C | Zou et al. | Song et al. | Shen & Huang |
| Coord. | Total pos. | 111.97 | 39.94 | 94.45 | 36.60 | 66.04 | 500.00 | 41.24 |
| | True pos. | 25.00 | 25.00 | 25.00 | 25.00 | 25.00 | 25.00 | 25.00 |
| | Sensitivity | 1.00 | 1.00 | 1.00 | 1.00 | 1.00 | 1.00 | 1.00 |
| | Specificity | 0.82 | 0.97 | 0.85 | 0.98 | 0.91 | 0.00 | 0.97 |
| | Matthews | 0.57 | 0.81 | 0.52 | 0.83 | 0.65 | 0.00 | 0.85 |
| Loading | Total pos. | 576.81 | 220.77 | 490.82 | 204.22 | 121.38 | 2004.37 | 73.31 |
| | True pos. | 119.63 | 120.00 | 120.00 | 120.00 | 73.47 | 95.06 | 53.30 |
| | Sensitivity | 1.00 | 1.00 | 1.00 | 1.00 | 0.61 | 0.79 | 0.44 |
| | Specificity | 0.81 | 0.96 | 0.84 | 0.96 | 0.98 | 0.20 | 0.99 |
| | Matthews | 0.50 | 0.71 | 0.46 | 0.73 | 0.59 | -0.00 | 0.56 |

Table S3: Measures of variable selection performance of the cross-validated estimates, based on the simulations for PCA model III. See text for description of the measures and methods involved. Shown are averages from 100 repetitions.

S3 Supplement to Section 4.2: Multiclass LDA

We report additional simulation results from the same simulation reported in Section 4.2 (in the main article).

S3.1 Variable selection performance

The variable selection performance is measured to investigate the coordinate-wise sparsity pattern of the estimates. We report the results from the cross-validated estimates in Table S4. In Table S4, it is seen that our methods tend to choose more variables than needed, but shows better sensitivity than other methods. Overall, both FastPOI-C and Gaynanova et al. (2016)’s method show better performances than other methods, and there is no clear winner among FastPOI-C and Gaynanova et al. (2016)’s.

S3.2 Extension of main article Tables 2 and 4

We report an extension of Tables 3 and 4, in the main article. We included the numerical results from two more choices of tuning parameter, $\tilde{\lambda}$ (for the ideal choice) and $\check{\lambda}$ (for minimizing misclassification rates), as well as using $\hat{\lambda}$ that maximizes the sum of predicted eigenvalues (our proposal). We briefly explain $\tilde{\lambda}$ and $\check{\lambda}$ below.

The ideal choice of tuning parameter is given by using $\mathbf{U}(\tilde{\lambda})$ where $\tilde{\lambda} = \arg \min_{\lambda \in L} \rho(\hat{\mathbf{U}}(\lambda), \mathbf{U})$ is chosen to minimize the distance to the true subspace.

Given that the classification is the goal of analysis, one could use a tuning set to directly tune the performance of the classification. To implement this alternative method of tuning λ , the multiclass LDA is trained for $\mathbf{X}\hat{\mathbf{U}}(\lambda)$ for each choice of λ . The tuned parameter $\check{\lambda}$ is the value of λ for which the misclassification error rate (MCE) of the tuning data set is the smallest. All three choices of tuning parameters are used for our methods (FastPOI-L and FastPOI-C) and the competing methods.

In Tables S5 and S6, the choice of λ by “Ideal” stands for $\tilde{\lambda}$, the ideal choice; by “Pred” we mean $\hat{\lambda}$; and by “MCE” we mean $\check{\lambda}$, minimizing the misclassification error rate. Numerical results in the tables are based on 100 repetitions. We note that our numerical results are similar to each other for different choices of tuning parameter. In particular, FastPOI-L solution has the smallest possible distance to truth, among all methods considered, for Models I–IV, and the performance of FastPOI-C from either choice of tuning is comparable.

| Number of total positives | | | | | |
|---------------------------|-----------|-----------|------------|-------------------|------------------|
| Model | FastPOI-L | FastPOI-C | Mai et al. | Clemmensen et al. | Gaynanova et al. |
| I | 11.90 | 10.61 | 12.45 | 9.10 | 8.52 |
| II | 112.25 | 14.91 | 94.88 | 6.85 | 6.31 |
| III | 17.23 | 12.23 | 9.40 | 7.75 | 8.76 |
| IV | 83.31 | 10.40 | 50.98 | 6.97 | 6.95 |
| V | 108.15 | 23.10 | 16.42 | 15.34 | 12.89 |

| Number of true positives | | | | | |
|--------------------------|-----------|-----------|------------|-------------------|------------------|
| Model | FastPOI-L | FastPOI-C | Mai et al. | Clemmensen et al. | Gaynanova et al. |
| I | 4.97 | 4.98 | 4.80 | 4.38 | 4.39 |
| II | 4.99 | 4.39 | 4.23 | 3.42 | 3.66 |
| III | 4.93 | 4.94 | 4.59 | 3.35 | 3.86 |
| IV | 3.85 | 3.61 | 2.95 | 3.30 | 3.02 |
| V | 4.99 | 4.87 | 3.09 | 4.88 | 4.32 |

| Sensitivity | | | | | |
|-------------|-----------|-----------|------------|-------------------|------------------|
| Model | FastPOI-L | FastPOI-C | Mai et al. | Clemmensen et al. | Gaynanova et al. |
| I | 0.99 | 1.00 | 0.96 | 0.88 | 0.88 |
| II | 1.00 | 0.88 | 0.85 | 0.68 | 0.73 |
| III | 0.99 | 0.99 | 0.92 | 0.67 | 0.77 |
| IV | 0.96 | 0.90 | 0.74 | 0.82 | 0.76 |
| V | 1.00 | 0.97 | 0.62 | 0.98 | 0.86 |

| Specificity | | | | | |
|-------------|-----------|-----------|------------|-------------------|------------------|
| Model | FastPOI-L | FastPOI-C | Mai et al. | Clemmensen et al. | Gaynanova et al. |
| I | 0.96 | 0.97 | 0.96 | 0.98 | 0.98 |
| II | 0.45 | 0.95 | 0.54 | 0.98 | 0.99 |
| III | 0.94 | 0.96 | 0.98 | 0.98 | 0.97 |
| IV | 0.59 | 0.97 | 0.75 | 0.98 | 0.98 |
| V | 0.47 | 0.91 | 0.93 | 0.95 | 0.96 |

| Matthews correlation coefficient | | | | | |
|----------------------------------|-----------|-----------|------------|-------------------|------------------|
| Model | FastPOI-L | FastPOI-C | Mai et al. | Clemmensen et al. | Gaynanova et al. |
| I | 0.75 | 0.79 | 0.69 | 0.69 | 0.72 |
| II | 0.14 | 0.56 | 0.20 | 0.59 | 0.66 |
| III | 0.61 | 0.72 | 0.80 | 0.55 | 0.69 |
| IV | 0.17 | 0.65 | 0.32 | 0.66 | 0.61 |
| V | 0.19 | 0.56 | 0.56 | 0.58 | 0.64 |

Table S4: Measures of variable selection performance, based on the simulations for MLDA models.

See text for description of the measures and methods involved. Shown are averages from 100 repetitions. The standard errors of each measure are at most 6.88, 0.13, 0.03, 0.04 and 0.02, respectively.

| Model | Choice of λ | FastPOI-L | FastPOI-C | Mai et al. | Clemmensen et al. | Gaynanova et al. |
|-------|---------------------|-----------|-----------|------------|-------------------|------------------|
| I | Ideal | 0.303 | 0.292 | 0.340 | 0.614 | 0.311 |
| | Pred. | 0.328 | 0.313 | 0.371 | 0.622 | 0.377 |
| | MCE | 0.366 | 0.342 | 0.406 | 0.630 | 0.389 |
| II | Ideal | 0.392 | 0.553 | 0.864 | 0.779 | 0.555 |
| | Pred. | 0.839 | 0.570 | 0.936 | 0.817 | 0.611 |
| | MCE | 0.797 | 0.605 | 0.914 | 0.858 | 0.607 |
| III | Ideal | 0.511 | 0.418 | 0.465 | 0.771 | 0.536 |
| | Pred. | 0.644 | 0.437 | 0.542 | 0.784 | 0.608 |
| | MCE | 0.634 | 0.468 | 0.516 | 0.806 | 0.612 |
| IV | Ideal | 0.372 | 0.437 | 0.854 | 0.662 | 0.451 |
| | Pred. | 0.852 | 0.478 | 0.916 | 0.689 | 0.514 |
| | MCE | 0.808 | 0.507 | 0.916 | 0.697 | 0.540 |
| V | Ideal | 0.381 | 0.323 | 0.823 | 0.333 | 0.289 |
| | Pred. | 0.712 | 0.359 | 0.869 | 0.365 | 0.411 |
| | MCE | 0.720 | 0.421 | 0.852 | 0.389 | 0.359 |

Table S5: The projection distance from the estimate, averaged from 100 repetitions, for sparse discriminant basis learning. The standard errors are at most 0.024. Smaller distance indicates more precise estimation.

| Model | Choice of λ | FastPOI-L | FastPOI-C | Mai et al. | Clemmensen et al. | Gaynanova et al. |
|-------|---------------------|-----------|-----------|------------|-------------------|------------------|
| I | Ideal | 7.28 | 7.15 | 7.75 | 10.08 | 7.24 |
| | Pred. | 7.46 | 7.27 | 9.41 | 10.23 | 12.30 |
| | MCE | 7.88 | 7.69 | 8.28 | 10.38 | 7.84 |
| II | Ideal | 37.67 | 8.60 | 23.72 | 10.79 | 9.16 |
| | Pred. | 30.50 | 8.72 | 21.74 | 9.70 | 12.49 |
| | MCE | 16.45 | 9.12 | 20.70 | 9.52 | 9.13 |
| III | Ideal | 22.65 | 12.19 | 14.40 | 18.03 | 15.63 |
| | Pred. | 17.10 | 12.41 | 17.23 | 18.41 | 19.19 |
| | MCE | 17.26 | 12.64 | 14.70 | 18.14 | 14.65 |
| IV | Ideal | 39.62 | 15.69 | 28.90 | 18.59 | 15.87 |
| | Pred. | 35.84 | 16.03 | 23.62 | 18.00 | 19.68 |
| | MCE | 28.59 | 16.39 | 23.84 | 18.49 | 15.91 |
| V | Ideal | 40.47 | 16.35 | 28.02 | 16.55 | 12.88 |
| | Pred. | 32.40 | 16.13 | 26.80 | 16.57 | 15.98 |
| | MCE | 22.69 | 14.90 | 23.56 | 16.65 | 13.16 |

Table S6: Misclassification rates (in percent) of the test set, averaged from 100 repetitions. The standard errors are at most 1.29. Smaller error rate indicates better classification.

S4 Supplement to Section 4.3: Sufficient dimension reduction

We provide numerical evidences for numerical instability of Chen et al. (2010)’s method and that our approach is much faster than Chen et al. (2010)’s.

In Table S7, we compare the average computation times needed to estimate the 2-dimensional sufficient subspace, computed from variants of sliced inverse regression (SIR). As the dimension p increases, the computation times for all methods also increase. The difference in computation times between SIR (Li, 1991) and SIR with POI-C (POI with coordinate-wise sparsity) is exactly the extra time needed to replace the standard generalized eigen-decomposition by the sparse generalized eigen-decomposition, computed using POI-C algorithm. Note that for rank-deficit cases, e.g. $(n, p) = (100, 100)$ or $(100, 500)$, both the standard and penalized estimation required more computation times than for the case with full-rank matrices. For those rank-deficit cases, Chen et al. (2010)’s method did not converge in an hour (3,600,000 milliseconds), so we had to terminate the process and omitted the result. Even when it converged for other cases, the computation times are about 100 times longer than POI-C.

| (n, p) | SIR | SIR with POI-C | Chen et al. |
|-------------|-------|----------------|----------------|
| (100, 10) | 3.22 | 2.99 | 537.81 |
| (100, 100) | 6.58 | 17.96 | Did not finish |
| (100, 500) | 62.85 | 904.33 | Did not finish |
| (1000, 10) | 2.83 | 3.02 | 335.17 |
| (1000, 100) | 5.50 | 10.15 | 3,488.63 |
| (1000, 500) | 43.15 | 119.89 | 104,579.02 |

Table S7: Sliced inverse regression for Tai-Chi data. Computation times in milliseconds (average of 10 trials). Computation was done using Matlab 2015 on a standard desktop computer (Intel i7-4770 CPU 2.40GHz with 16 gigabytes of RAM). Both SIR and Chen et al. (2010)’s method were implemented using the Matlab package of Coordinate-independent Sparse Estimation (Chen, 2018).

In Table S8, we compare the average accuracy of the estimated sufficient subspace. Note that SIR with POI-C have perfectly recovered the true subspace in all situations. While

Chen et al. (2010)’s method sometimes exhibits the exact recovery of true subspace, the algorithm is highly unstable. This can be seen in the table for $p = 10$, in which cases, the iterated solution of Chen et al. (2010) seemed to have converged to a local optimum, for roughly a half of time.

| (n, p) | SIR | SIR with POI-C | Chen et al. |
|-------------|------|----------------|----------------|
| (100, 10) | 0.98 | 0.00 | 0.89 |
| (100, 100) | 1.00 | 0 | Did not finish |
| (100, 500) | 1.00 | 0 | Did not finish |
| (1000, 10) | 0.96 | 0.00 | 0.60 |
| (1000, 100) | 0.99 | 0.00 | 0.00 |
| (1000, 500) | 1.00 | 0.00 | 0.00 |

Table S8: Sliced inverse regression for Tai-Chi data. Projection distance from the estimates, averaged from 10 trials.

S5 Supplement to Section 4.4: Canonical correlation analysis

We provide the model and simulation setting used in sparse estimation of canonical correlation analysis (CCA) and the numerical results.

We borrow the model used in Safo et al. (2018). In particular, the concatenated random vector $\mathbf{z}^T = (\mathbf{x}^T, \mathbf{y}^T)$ follows the multivariate normal distribution with mean $\mathbf{0}$ and covariance matrix

$$\Sigma = \begin{pmatrix} \Sigma_1 & \Sigma_{12} \\ \Sigma_{12}^T & \Sigma_2 \end{pmatrix}.$$

For $0 \leq \rho < 1$ and a natural number s , let $C_s(\rho) = (1 - \rho)\mathbf{I}_s + \rho\mathbf{J}_s$, $\mathbf{J}_s = \mathbf{1}_s\mathbf{1}_s^T$. We set Σ_1 as the block diagonal matrix of $C_{20}(.7)$ and \mathbf{I}_{180} , Σ_2 as the block diagonal matrix of $C_{15}(.7)$ and \mathbf{I}_{135} , and Σ_{12} as the block diagonal matrix of $.6\mathbf{1}_{20}\mathbf{1}_{15}^T$ and $\mathbf{0}_{180 \times 135}$. Under this model, there is only one canonical pair $(\mathbf{g}, \mathbf{h}) \in \mathbb{R}^{200} \times \mathbb{R}^{150}$ in which only first 10% of coefficients are nonzero. The true canonical correlation is approximately $\rho = 0.8362$. This model corresponds to Setting I in Safo et al. (2018).

We applied the POI. Note that since there is only one vector to evaluate, POI-L is the

same as to POI-C. The performances in estimating (\mathbf{g}, \mathbf{h}) and ρ are evaluated separately, using the measures defined in Section S2, based on 100 repetition. We also directly compare the performance of Gao et al. (2017)’s method. These are contained in Table S9. Safo et al. (2018) reported that their proposed method, called “SELP-I” performed the best in the Setting I of the paper, compared to methods of Gao et al. (2017), Witten et al. (2009), Parkhomenko et al. (2009) and Chalise and Fridley (2012). For reference we also list the numerical results of “SELP-I” in Table S9. In this setting, our method has a potential to provide much more accurate estimates. Our estimate using the proposed tuning procedure performs inferior in terms of accuracy to “SELP-I” of Safo et al. (2018), but shows a similar performance in terms of variable selection and canonical correlation estimation. Both our methods and Safo et al.’s performed much better than those of Gao et al. (2017), Witten et al. (2009), Parkhomenko et al. (2009) and Chalise and Fridley (2012).

| | | POI (min) | POI (CV) | Gao et al. | Safo et al. |
|----------|---------------------|-----------|----------|------------|-------------|
| α | Projection distance | 0.135 | 0.239 | 0.997 | 0.144 |
| | Sensitivity | 1.000 | 1.000 | 0.749 | 1.000 |
| | Specificity | 0.975 | 0.968 | 0.920 | 0.993 |
| | Matthews | 0.907 | 0.902 | 0.642 | 0.964 |
| β | Projection distance | 0.129 | 0.225 | 0.994 | 0.144 |
| | Sensitivity | 1.000 | 1.000 | 0.711 | 1.000 |
| | Specificity | 0.976 | 0.962 | 0.923 | 0.988 |
| | Matthews | 0.910 | 0.895 | 0.624 | 0.945 |
| | $\hat{\rho}$ | 0.838 | 0.847 | 0.904 | 0.839 |

Table S9: Performance in sparse CCA by the POI. POI (min) refers to the choice of tuning parameter by the minimum distance to truth; POI (CV) refers to the choice of tuning parameter by using the proposed cross validation procedure. The largest standard errors are 0.1, 0.26, 0.11, 0.21, 0.05 for Projection distance, Sensitivity, Specificity, Matthews correlation coefficient and $\hat{\rho}$, respectively.

S6 Supplement to Section 4: Genomic data analysis

We report an application of the proposed method in the exploratory data analysis of a large-scale genomic data. The data set was introduced in Ciriello et al. (2015), and consists of

16,615 gene expression levels measured for 817 breast cancer tumor samples. These tumor samples were pre-classified by a pathology committee, and grouped into five subtypes of lobular breast cancer—Luminal A, Basal-like, Luminal B, HER2-enriched, and normal-like. For this dataset, we apply sparse PCA and multiclass LDA using the proposed POI algorithm.

S6.1 Feature selection by sparse principal component analysis

We first used the data to understand the behavior of sparse PCA estimates by the POI. For this study, we kept the 500 variables with the largest standard deviations, and added to each observation 500 noise variables, sampled from the standard normal distribution. For any “sparse” estimation methods in this context, the estimated basis vectors should not include the 500 noise variables. To evaluate the performance in the smaller sample size situation, we use one third of the sample, consisting of $n = 272$ observations. The data are then standardized (so that each variable has mean zero and unit variance).

For this data set of size $(n, p) = (272, 1000)$, we use the POI with coordinate-wise sparse penalty (POI-C) with the tuning parameter given by $\lambda = \lambda_{\max}/2$ in estimation of principal subspace of dimension d . To glimpse the stability of the estimates against varying dimension d , we have repeated the analysis for $d = 1$ to $d = 20$, and have collected the estimated eigenvalues and eigenvectors. The result of analysis is graphically summarized in Fig. S1, which also appears in the main article.

In Fig. S1, notice that the estimated eigenvalues (shown in the left panel) are slowly decreasing but are stable across a range of d . It appears that the first three or four largest eigenvalue estimates “stand out” among others, indicating a potentially small number of true principal components.

In the middle panel, the sparsity patterns of estimated eigenspaces are shown. As desired, the latter 500 coordinates are estimated to be zero. Moreover, the number of nonzero coordinates seems to be stable as d increases.

The right panel of Fig. S1 shows the absolute value of the inner product between $\hat{\mathbf{q}}_{i,i}$ and $\hat{\mathbf{q}}_{i,d}$ for $d \geq i$, where $\hat{\mathbf{q}}_{i,d}$ is the i th principal component (PC) direction vector when estimating d PCs. For clarity, we show the first three PC directions, and they are stable against increasing d .

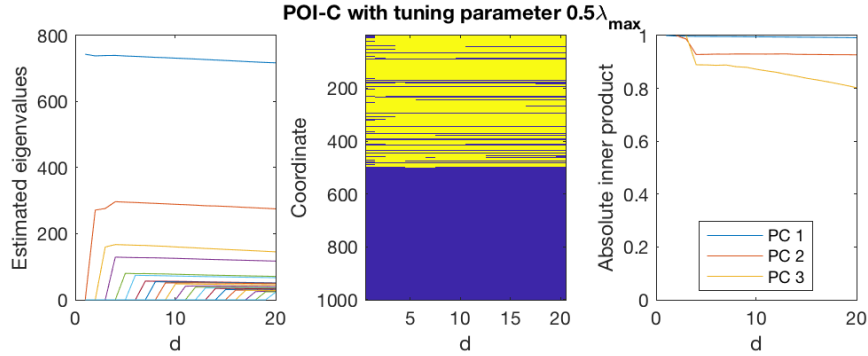


Figure S1: Sparse principal component analysis by POI with coordinate-wise sparse penalty for the genomic data set. The analysis is repeated for subspace dimension $d = 1$ to 20. Shown are estimated eigenvalues (left), nonzero coordinates shown as lighter color (middle) and $|\hat{\mathbf{q}}_{i,i}^T \hat{\mathbf{q}}_{i,d}|$ for $i = 1, 2, 3$ (right).

S6.2 Linear classification

We now demonstrate the application of Fast POI in learning sparse discriminant basis from the data.

The data were split in half at random, where the first half with 409 cases was used for training, and the other half was used for testing. We kept the 2,000 variables with the largest standard deviations, and then standardized the data (so that each variable has mean zero and unit variance). The \mathbf{B} and \mathbf{A} matrices were then prepared by the sample estimates of the within-group and between group covariance matrices, Σ_W and Σ_B , respectively. For this large data, sparse estimation of the generalized eigenvectors by Fast POI algorithms took only 2.09 seconds on average over a range of λ (on a standard Macbook). This is much faster than, e.g., estimating by Clemmensen et al. (2011)’s method (using the `spaSM` package, Sjöstrand et al., 2012) which took about a minute.

We further considered applying our methods to linear classification. For this experiment, the data were divided into three equal-sized groups: training, tuning and testing sets of size 272. Due to heavy-computation cost (mostly from using the `spaSM` package), only the 500 variables with the largest raw standard deviations were kept. We compared FastPOI-L, FastPOI-C, Mai et al. (2017)’s method, Clemmensen et al. (2011)’s method and Gaynanova et al. (2016)’s method, as used in the simulation study in the main article Section 4.2 .

The training set was used to estimate the subspace $\hat{\mathbf{U}}$, while the tuning set was used

| | Pred. | | MCE | |
|-------------------|--------------|---------------|--------------|---------------|
| | Error | #Signal | Error | #Signal |
| FastPOI-L | 17.86 (0.23) | 303.2 (58.2) | 18.35 (0.19) | 327.2 (129.5) |
| FastPOI-C | 16.64 (0.19) | 205.1 (45.5) | 17.25 (0.19) | 235.4 (126.1) |
| Mai et al. | 17.40 (0.20) | 311.6 (83.8) | 17.36 (0.20) | 365.3 (142.3) |
| Clemmensen et al. | 17.89 (0.20) | 218.2 (49.8) | 18.21 (0.21) | 199.9 (99.9) |
| Gaynanova et al. | 22.64 (9.49) | 83.37 (65.39) | 18.06 (1.99) | 79.4 (36.8) |

Table S10: Basis learning for classification on the lobula breast cancer data. Column “Error” contains the means (standard errors) of the misclassification rates (in percent) of the test data set. Column “#Signal” contains the means (standard deviations) of the number of non-zero coordinates in the estimated basis. Data are randomly split for 100 times. “Pred” and “MCE” refer to the cross-validation method used.

to compute the cross-validation score. The testing set was used to compute estimates of misclassification rate. The tuning parameters were chosen by two different standards: one maximizing the predicted sum of eigenvalues, and one minimizing the tuning classification error. The performances of classification are summarized in Table S10. The results are mixed. All methods turn out to be equally well-performing. On the other hand, Gaynanova’s method provides the smallest number of non-zero coordinates in the estimated eigenvector matrix.

References

- Allen, G. I., L. Grosenick, and J. Taylor (2014). A generalized least-square matrix decomposition. *Journal of the American Statistical Association* 109(505), 145–159.
- Bouveyron, C., P. Latouche, and P.-A. Mattei (2016). Bayesian variable selection for globally sparse probabilistic PCA. Preprint HAL 01310409, Université Paris Descartes. arXiv:1605.05918.
- Cai, T. and W. Liu (2011). A direct estimation approach to sparse linear discriminant analysis. *Journal of the American Statistical Association* 106(496), 1566–1577.

- Chalise, P. and B. L. Fridley (2012). Comparison of penalty functions for sparse canonical correlation analysis. *Computational Statistics and Data Analysis* 56, 245–254.
- Chen, M., C. Gao, Z. Ren, and H. H. Zhou (2018). Sparse cca via precision adjusted iterative thresholding. In L. Y. Shing-Tung Yau and S.-Y. Cheng (Eds.), *Proceedings of International Congress of Chinese Mathematicians*, Volume to appear.
- Chen, X. (2018). Matlab package for Coordinate-independent Sparse Estimation. Web link at <https://www.stat.nus.edu.sg/stacx/cise.zip>, retrieved on May 25, 2018.
- Chen, X., C. Zou, R. D. Cook, et al. (2010). Coordinate-independent sparse sufficient dimension reduction and variable selection. *The Annals of Statistics* 38(6), 3696–3723.
- Ciriello, G., M. L. Gatzka, A. H. Beck, M. D. Wilkerson, S. K. Rhie, A. Pastore, H. Zhang, M. McLellan, C. Yau, C. Kandath, et al. (2015). Comprehensive molecular portraits of invasive lobular breast cancer. *Cell* 163(2), 506–519.
- Clemmensen, L., T. Hastie, D. Witten, and B. Ersbll (2011). Sparse discriminant analysis. *Technometrics* 53(4), 406–413.
- Cook, R. D. (2009). *Regression graphics: Ideas for studying regressions through graphics*, Volume 482. John Wiley & Sons.
- d’Aspremont, A., F. Bach, and L. E. Ghaoui (2008). Optimal solutions for sparse principal component analysis. *Journal of Machine Learning Research* 9(Jul), 1269–1294.
- Gao, C., Z. Ma, H. H. Zhou, et al. (2017). Sparse cca: Adaptive estimation and computational barriers. *The Annals of Statistics* 45(5), 2074–2101.
- Gaynanova, I., J. G. Booth, and M. T. Wells (2016). Simultaneous sparse estimation of canonical vectors in the $p \gg n$ setting. *Journal of the American Statistical Association* 111(514), 696–706.
- Hyvärinen, A., J. Karhunen, and E. Oja (2004). *Independent component analysis*, Volume 46. John Wiley & Sons.
- Jenatton, R., G. Obozinski, and F. Bach (2010). Structured sparse principal component analysis. In *Proceedings of the Thirteenth International Conference on Artificial Intelligence and Statistics*, pp. 366–373.

- Jolliffe, I. T., N. T. Trendafilov, and M. Uddin (2003). A modified principal component technique based on the lasso. *Journal of computational and Graphical Statistics* 12(3), 531–547.
- Kokiopoulou, E., J. Chen, and Y. Saad (2011). Trace optimization and eigenproblems in dimension reduction methods. *Numerical Linear Algebra with Applications* 18(3), 565–602.
- Li, G. and S. Jung (2017). Incorporating covariates into integrated factor analysis of multi-view data. *Biometrics* 73(4), 1433–1442.
- Li, K.-C. (1991). Sliced inverse regression for dimension reduction (with discussion). *Journal of the American Statistical Association* 86(414), 316–342.
- Li, L. (2007). Sparse sufficient dimension reduction. *Biometrika* 94(3), 603–613.
- Lock, E. F., K. A. Hoadley, J. S. Marron, and A. B. Nobel (2013). Joint and individual variation explained (jive) for integrated analysis of multiple data types. *The Annals of Applied Statistics* 7(1), 523.
- Ma, Z. (2013). Sparse principal component analysis and iterative thresholding. *The Annals of Statistics* 41(2), 772–801.
- Mai, Q., Y. Yang, and H. Zou (2017). Multiclass sparse discriminant analysis. *Statistica Sinica* (to appear). arXiv:1504.05845.
- Mai, Q., H. Zou, and M. Yuan (2012). A direct approach to sparse discriminant analysis in ultra-high dimensions. *Biometrika* 99(1), 29–42.
- Parkhomenko, E., D. Tritchler, and J. Beyene (2009). Sparse canonical correlation analysis with application to genomic data integration. *Statistical Applications in Genetics and Molecular Biology* 8.
- Safo, S. E., J. Ahn, Y. Jeon, and S. Jung (2018). Sparse generalized eigenvalue problem with application to canonical correlation analysis for integrative analysis of methylation and gene expression data. *Biometrics in press*.
- Shao, J., Y. Wang, X. Deng, and S. Wang (2011). Sparse linear discriminant analysis by thresholding for high dimensional data. *The Annals of statistics*, 1241–1265.

- Shen, D., H. Shen, and J. S. Marron (2013). Consistency of Sparse PCA in High Dimension , Low Sample Size Contexts. *Journal of Multivariate Analysis* 115, 317—333.
- Shen, H. and J. Z. Huang (2008). Sparse principal component analysis via regularized low rank matrix approximation. *Journal of multivariate analysis* 99(6), 1015–1034.
- Sjöstrand, K., L. H. Clemmensen, R. Larsen, and B. Ersbøll (2012). Spasm: A matlab toolbox for sparse statistical modeling. *URL www2.imm.dtu.dk/projects/spasm/*.
- Song, J., P. Babu, and D. P. Palomar (2015). Sparse generalized eigenvalue problem via smooth optimization. *IEEE Transactions on Signal Processing* 63(7), 1627–1642.
- Tyler, D. E., F. Critchley, L. Dümbgen, and H. Oja (2009). Invariant co-ordinate selection. *Journal of the Royal Statistical Society: Series B (Statistical Methodology)* 71(3), 549–592.
- Van Loan, C. F. (1976). Generalizing the singular value decomposition. *SIAM Journal on Numerical Analysis* 13(1), 76–83.
- Witten, D. and R. Tibshirani (2011). Penalized classification using fisher’s linear discriminant. *Journal of the Royal Statistical Society: Series B (Statistical Methodology)* 73(5), 753–772.
- Witten, D. M., R. Tibshirani, and T. Hastie (2009). A penalized matrix decomposition, with applications to sparse principal components and canonical correlation analysis. *Bio-statistics* 10(3), 515–534.
- Zou, H., T. Hastie, and R. Tibshirani (2006). Sparse principal component analysis. *Journal of Computational and Graphical Statistics* 15(2), 265–286.